Journal of Medicinal Chemistry

Article

Structure-Activity Relationship Studies of Mitogen Activated Protein Kinase Interacting Kinase (MNK) 1 & 2 and BCR-ABL1 Inhibitors Targeting Chronic Myeloid Leukemic Cells

Joseph Cherian, Kassoum Nacro, Zhi Ying Poh, Samantha Guo, Duraiswamy Athisayamani Jeyaraj, Yun Xuan Wong, Melvyn Ho, Hai Yan Yang, Joma Kanikadu Joy, Zekui Perlyn Kwek, Boping Liu, John Liang Kuan Wee , Esther HQ Ong, Meng Ling Choong, Anders Poulsen, May Ann Lee, Vishal Pendharkar, Li Jun Ding, Vithya Manoharan, Yun Shan Chew, Kanda Sangthongpitag, Sharon Lim, S. Tiong Ong, Jeffrey Hill, and Thomas H. Keller

J. Med. Chem., **Just Accepted Manuscript** • DOI: 10.1021/acs.jmedchem.5b01712 • Publication Date (Web): 24 Mar 2016

Structure-Activity Relationship Studies of Mitogen Activated Protein Kinase Interacting Kinase (MNK) 1 & 2 and BCR-ABL1 Inhibitors Targeting Chronic Myeloid Leukemic Cells

Joseph Cherian,[‖] Kassoum Nacro,[‖] Zhi Ying Poh,[‖] Samantha Guo,[‖,§] Duraiswamy A. Jeyaraj,[‖,‡] Yun Xuan Wong,[‖] Melvyn Ho,[‖,¶] Hai Yan Yang,[‖] Joma Kanikadu Joy,[‖] Zekui Perlyn Kwek,[‖] Boping Liu,[‖] John Liang Kuan Wee,[‖] Esther HQ Ong,[‖] Meng Ling Choong,[‖] Anders Poulsen,[‖] May Ann Lee,[‖] Vishal Pendharkar,[‖] Li Jun Ding,[‖] Vithya Manoharan,[‖] Yun Shan Chew,[‖] Kanda Sangthongpitag,[‖] Sharon Lim,[ϕ] S. Tiong Ong,[ϕ] Jeffrey Hill,[‖] Thomas H. Keller[‖]*

[‖] *Experimental Therapeutics Centre, 13 Biopolis Way, Nanos, Singapore 13866;*

[ϕ] *Duke-NUS Graduate Medical School, 8 College Road, Singapore.*

KEYWORDS: Blast Crisis, Chronic Myeloid Leukemia, Leukemic stem cells, self-renewal, MNK kinase, BCR-ABL1.

ABSTRACT

Clinically used BCR-ABL1 inhibitors for the treatment of chronic myeloid leukemia (CML) do not eliminate leukemic stem cells (LSC). It has been shown that MNK1 & 2 inhibitors prevent phosphorylation of eIF4E and eliminate the self-renewal capacity of LSCs. Herein, we describe the identification of novel dual MNK1 & 2 and BCR-ABL1 inhibitors, starting from the known kinase inhibitor **2**. Initial SAR studies resulted in compound **27** with loss of BCR-ABL1 inhibition. Further modification led to orally bioavailable dual MNK1 & 2 and BCR-ABL1 inhibitors **53** and **54**, which are efficacious in a mouse xenograft model and also reduce the level of phosphorylated eIF4E in the tumor tissues. Kinase selectivity of these compounds is also presented.

INTRODUCTION

Serine/threonine kinases MNK1 and MNK2 phosphorylate eukaryotic translation initiation factor 4E (eIF4E) at Ser209 and regulate the translation initiation.[1,2] Overexpression of eIF4E and its phosphorylated form have been shown to be responsible for abnormal growth and proliferation of breast,[3] prostate,[4] head and neck cancer cells[5] as well as blast crisis chronic myeloid leukemia (BC CML) cells.[6] It has been shown that in BC CML, overexpression of eIF4E and its phosphorylated form gives self-renewal capacity to blast crisis granulocyte macrophage progenitors (GMPs), allowing them to function as leukemic stem cells (LSCs).[6] While phosphorylation of eIF4E is necessary for oncogenic transformation,[4, 7] the kinase activity of MNK1 & 2 seems dispensable for normal development[1] making MNK1 & 2 kinases attractive anticancer targets.

Inhibition of MNK1 and MNK2 using **1** (CGP57380)[6] has been shown to be effective in preventing the phosphorylation of eIF4E as well as self-renewal of LSCs *in vitro* and *in vivo*.[6] However, the antiproliferative effect of **1** on BC CML cells was observed at doses higher than 10

μM, probably due to its weak BCR-ABL1 inhibition.[9] While clinical BCR-ABL1 inhibitors exhibit very good antiproliferative activity against actively dividing progenitors, they do not eliminate LSCs.[6,10-14] 4-[(4-Methylpiperazin-1-yl)methyl]-*N*-(4-methyl-3-{[4-(pyridin-3-yl)pyrimidin-2-yl]amino}phenyl)benzamide (imatinib)[15] and *N*-(2-chloro-6-methylphenyl)-2-[[6-[4-(2-hydroxyethyl)-1-piperazinyl]-2-methyl-4-pyrimidinyl]amino]-5-thiazole carboxamide (dasatinib)[16] do not inhibit MNK1 & 2 enzymes and had little effect in reducing the serial replating efficiency of LSCs at clinically relevant concentrations.[6] Combination of BCR-ABL1 inhibitor 4-methyl-*N*-[3-(4-methyl-1*H*-imidazol-1-yl)- 5-(trifluoromethyl)phenyl]-3- [(4-pyridin-3-ylpyrimidin-2-yl) amino]benzamide (nilotinib)[17] and JAK1/2 inhibitor (3*R*)-3-cyclopentyl-3-[4-(7*H*-pyrrolo[2,3-d]pyrimidin-4-yl)pyrazol-1-yl]propanenitrile (ruxolitinib)[18] was successful in preventing the self-renewal capacity of LSCs *in vitro* and *in vivo*, with some degree of toxicity to normal stem cells.[19] As MNK1 & 2 inhibitors were able to prevent self-renewal of LSCs, we envisaged that a single agent inhibitor of both BCR-ABL1 and MNK1 & 2 may be able to cause BC-CML cell death through the inhibition of BCR-ABL and block the self-renewal capacity of LSCs by inhibiting phosphorylation of eIF4E. Such an agent should be able to distinguish between normal stem cells and LSCs to minimize toxicity.

In addition to **1**,[20] other known MNK inhibitors include: **2** (AST-487)[21], **3** (staurosporine)[21] and **4** (cercosporamide)[22] (Figure 1) while a few other inhibitors have also appeared in the recent literature.[9,23,24] **2** and **4** have been shown to inhibit the phosphorylation of

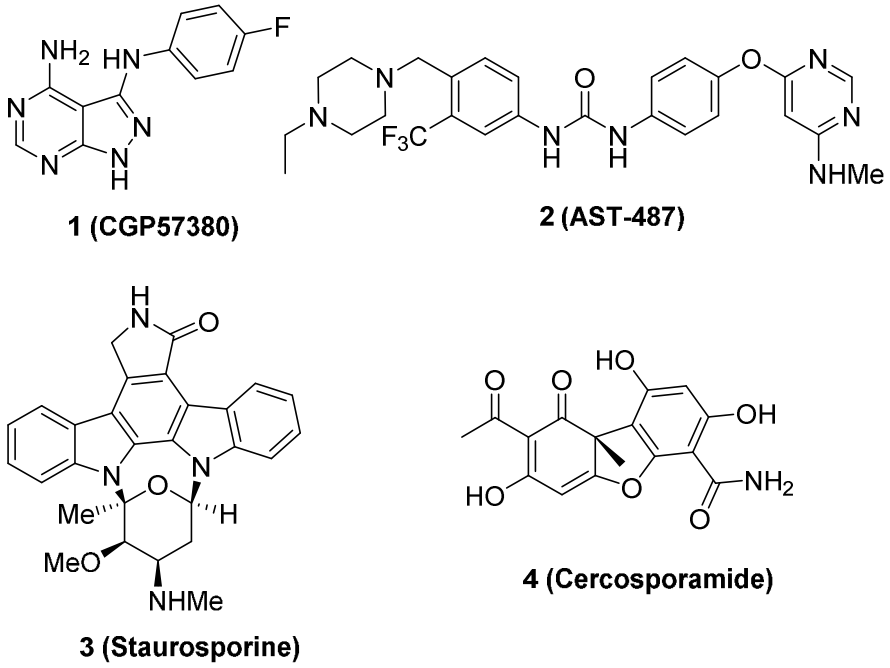

Figure 1: Examples of MNK1 and MNK2 inhibitors known in the literature

eIF4E and prevent self-renewal capacity of LSCs.[6] However, **2** is a multi-kinase inhibitor[21] and has been shown to influence self-renewal capacity of hematopoietic stem cells (HSCs), thus making it toxic towards normal HSCs. We used **2** as a starting point for the identification of novel inhibitors of MNK1, MNK2 and BCR-ABL1 that are non-toxic to HSCs.

CHEMISTRY:

2 was synthesized as previously reported.[25] Scheme 1 describes synthesis of **9** from **5**. Reduction of the methyl ester group of **5** was carried out using lithium aluminium hydride to furnish **6**. Subsequent treatment of the primary alcohol **6** with $MsCl/Et_3N$ followed by NaCN in DMSO and hydrolysis of the resulting nitrile intermediate furnished the required carboxylic acid **7**. Amide coupling of **7** with the previously reported aniline **8**[25] using $HBTU/Et_3N$ gave **9**.

Scheme 1: Synthesis of compound **9**.

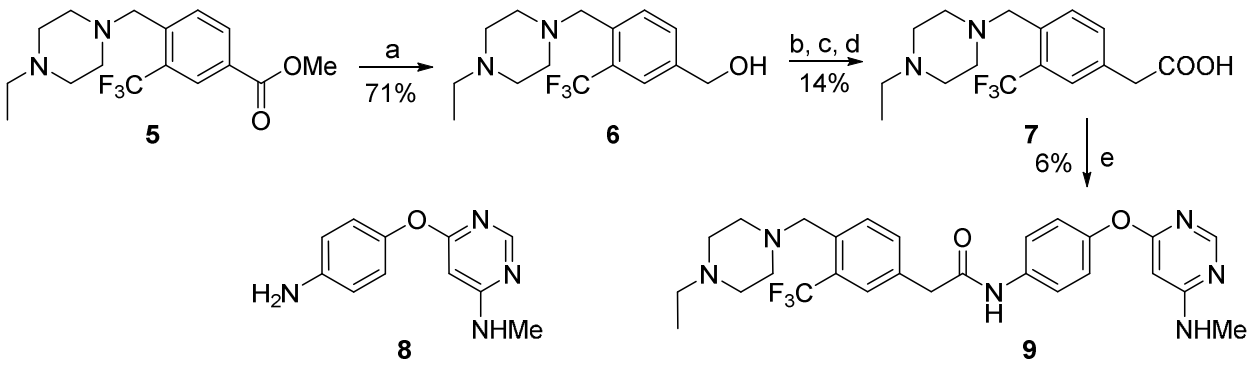

a) $LiAlH_4$, THF, 0 ^oC- rt, 4 h; b) MsCl, Et_3N, CH_2Cl_2; 0 ^oC – rt, 16 h; c) NaCN, DMSO, 90 ^oC, 14 h; d) 6N HCl, 90 ^oC, 16 h; e) **8**, HBTU, Et_3N, DMF, 16 h, rt.

Scheme 2: Synthesis of compounds **15**-**17**.

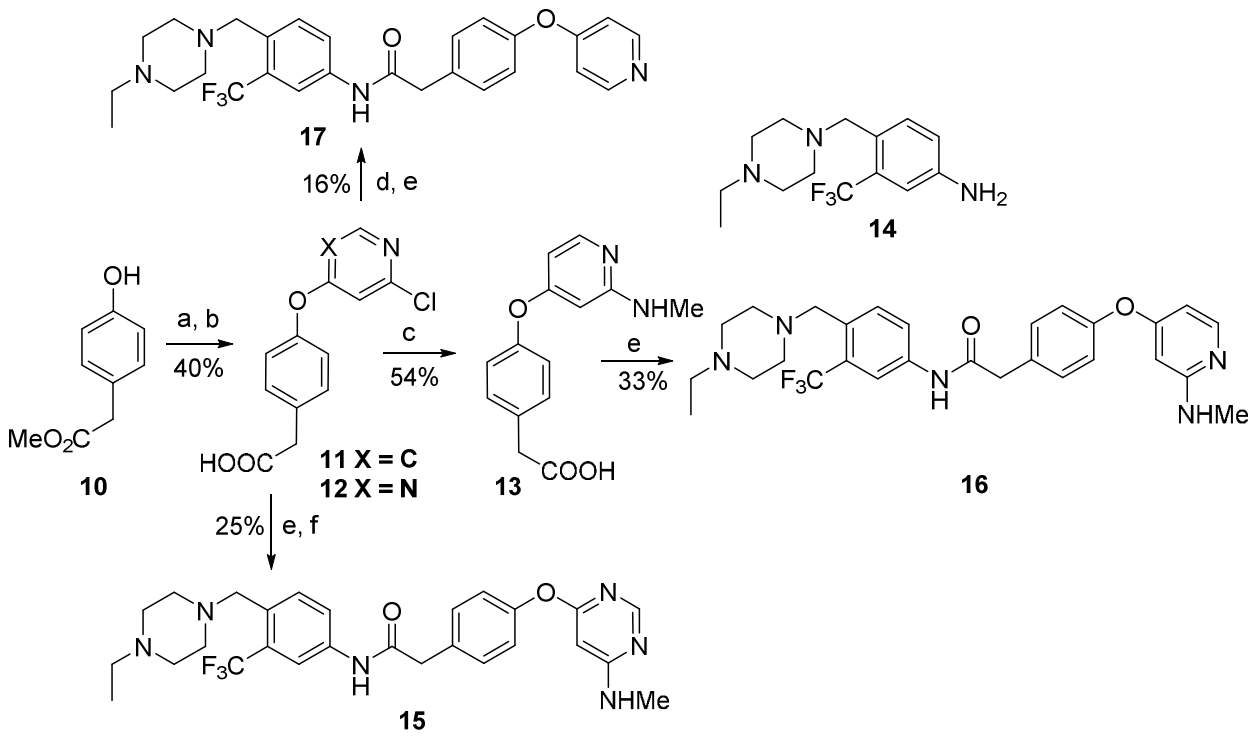

a) 2,4-dichloropyridine, K_2CO_3, DMF, 90 ^oC, 16 h; b) LiOH, THF-water, rt, 14 h; c) aq. $MeNH_2$, THF, 80 ^oC, 15 h; d) Pd/C/H_2, rt; e) **14**, HATU, Et_3N, DMF, rt; f) $MeNH_2$, THF, 80 ^oC, 16 h.

Scheme 2 depicts synthesis of **15 -17**. Methyl 2-(4-hydroxyphenyl)acetate **10** was converted to **11** by reacting with 2,4-dichloropyridine in presence of K_2CO_3 in DMF followed by ester hydrolysis using LiOH. In a similar manner, **12**[26] was synthesized from **10** using 4,6-dichloropyrimidine. **11** was converted to **13** by treatment with aq. $MeNH_2$ in THF. Coupling of **12** with **14** using HATU/Et_3N followed by reacting with $MeNH_2$ resulted in the formation of **15**. Coupling of the acid **13** and previously reported aniline **14**[25] using HATU/Et_3N gave **16**. Hydrodehalogenation of the monochloro intermediate **11** over Pd/C under H_2 followed by coupling with aniline **14** under previously mentioned conditions resulted in **17**.

Converting **19** to the corresponding acid chloride and subsequent reaction with **14** and **18** gave intermediates **24** and **25** (Scheme 3). Coupling of anilines **14** and **18** with commercially available carboxylic acids **20-23** resulted in compounds **26-29**. Intermediate **24** was subjected to Suzuki coupling with (6-acetamidopyridin-3-yl)boronic acid to provide compound **30**. **25** was converted to **31** by Suzuki coupling reaction with pyridine-3-boronic acid and subsequent *N*-boc deprotection.

Scheme 3: Synthesis of compounds **26-31**.

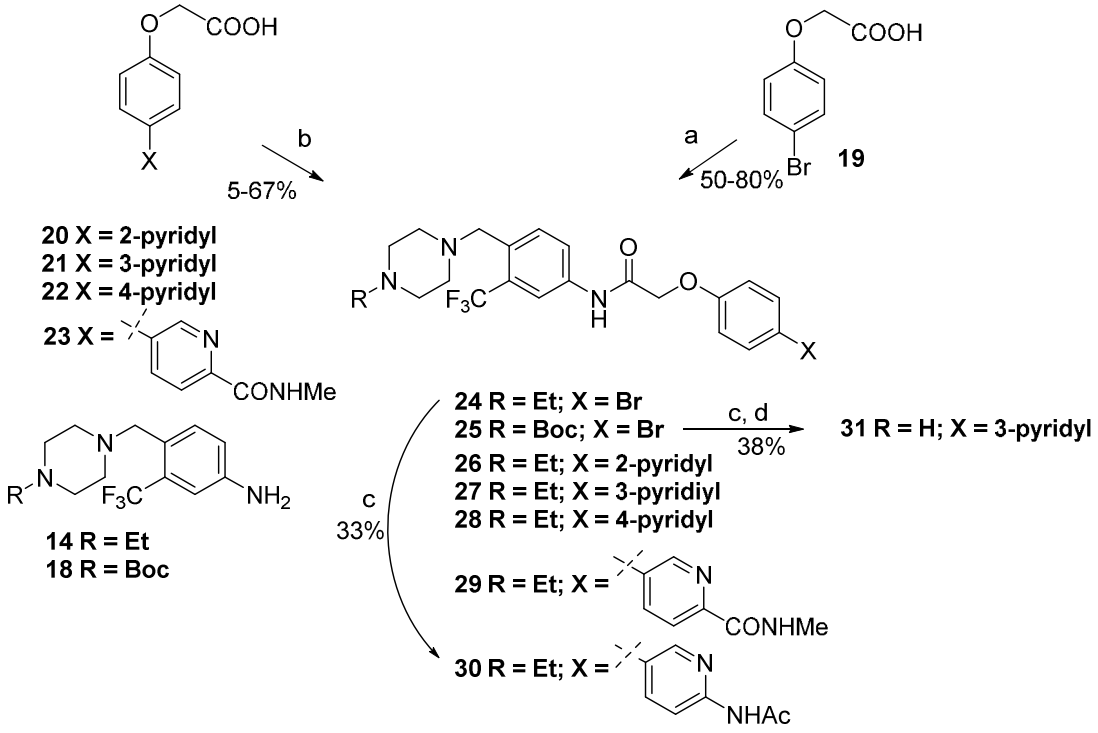

a) $(COCl)_2$, DMF, CH_2Cl_2 0 ^oC-1 h followed by Et_3N, **14** or **18**, rt, 16 h; b) HBTU, Et_3N, DMF, **14** or **18**, rt; c) K_3PO_4, $Pd_2(dba)_3$, PCy_3, (6-acetamidopyridin-3-yl)boronic acid for **30** and pyridine-3-boronic acid for **31**, dioxane-water, 100 ^oC; d) TFA, CH_2Cl_2.

Synthesis of **35** is depicted in Scheme 4. Reductive amination of **33** with **32** using $NaBH_3CN$ followed by coupling with 2-(4-bromophenoxy)acetic acid **19** using HATU/DIPEA in THF gave **34**. Suzuki coupling of **34** with pyridine-3-boronic acid resulted in compound **35**.

Scheme 4: Synthesis of compound **35**.

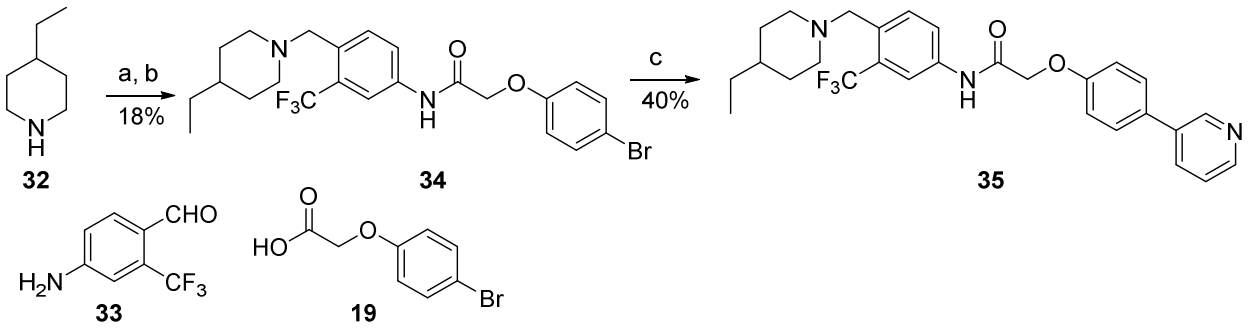

a) **33**, $NaBH_3CN$, AcOH, MeOH-THF, rt, 16 h; b) **19**, HATU, DIPEA, THF, rt, 2 h; c) $Pd_2(dba)_3$, PCy_3, K_3PO_4, Pyridine-3-boronic acid, dioxane-water, 100 ^oC, 16 h.

Arbuzove reaction of **36** with triethylphosphite and subsequent Wittig-Horner reaction of the resulting phosphonate with *N*-ethylpiperidin-4-one gave **37** (Scheme 5). Hydrogenation and subsequent coupling with 2-(4-(pyridin-3-yl)phenoxy)acetic acid yielded **38**.

Scheme 5: Synthesis of compound **38**.

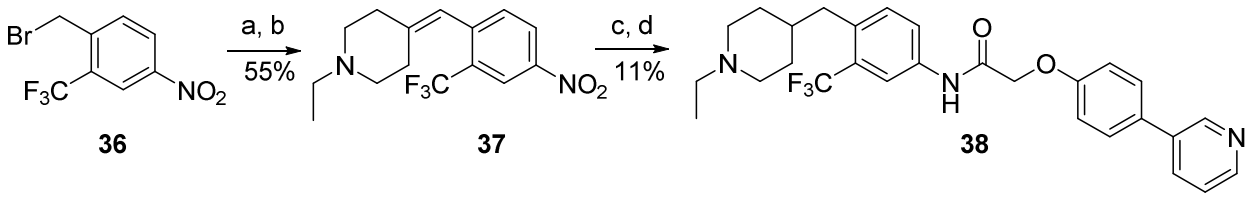

a) $P(OEt)_3$, Toluene, 100 ^oC, 16 h; b) 1-ethylpiperidin-4-one, NaH, THF, rt, 16 h; c) H_2, 50 psi, Pt/C, EtOH, 5 h; d) 2-(4-(pyridin-3-yl)phenoxy)acetic acid, HATU, DIPEA, DMF, 16 h, rt.

Suzuki coupling reaction between **39** and cyclopropylboronic acid, reduction of the nitro group using $NiCl_2.6H_2O/NaBH_4$ in MeOH followed by HATU/DIPEA mediated coupling with 2-(4-(pyridin-3-yl)phenoxy)acetic acid gave **40** (Scheme 6).

Scheme 6: Synthesis of compound **40**.

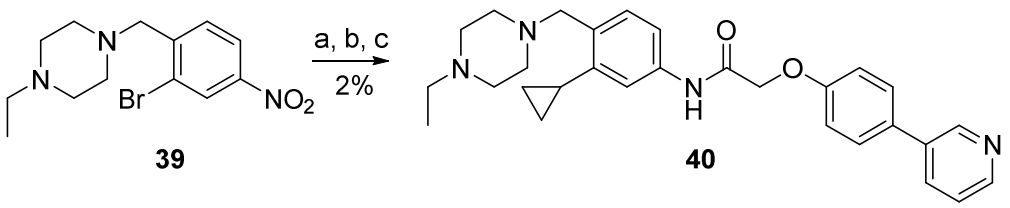

a) Cyclopropylboronic acid, $Pd(dppf)Cl_2.CH_2Cl_2$, dioxane, aq. K_2CO_3, 100 ^oC, 16 h; b) $NiCl_2.6H_2O$, $NaBH_4$, MeOH, 0 ^oC-rt, 4 h; c) 2-(4-(pyridin-3-yl)phenoxy)acetic acid, HATU, DIPEA, THF, rt, 6 h.

Suzuki coupling of **41**[27] with pyridine-3-boronic acid and subsequent coupling of the resulting carboxylic acid intermediate with aniline **14** under HATU/Et_3N/DMF condition gave **42** (Scheme 7).

Scheme 7: Synthesis of compound **42**.

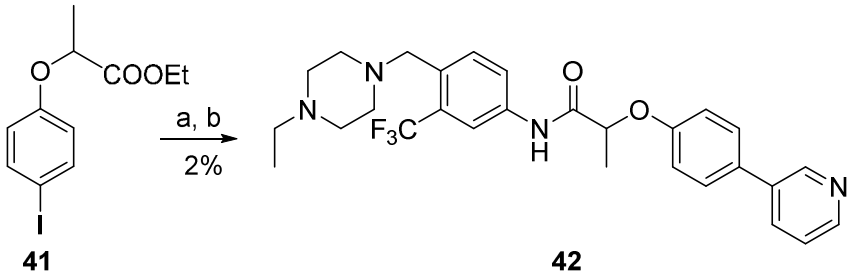

41 **42**

a) Pyridine-3-boronic acid, $Pd(PPh_3)_4$, Na_2CO_3, dioxane-water, 100 ^oC, 16 h; b) **14**, HATU, Et_3N, DMF, rt, 1.5 h.

Intermediates **46** and **47** were obtained by coupling of anilines **14** and **18** with **44.** Suzuki coupling of **46** and **47** with corresponding boronic acid or boronate esters (pyridine-3-boronic acid, (6-acetamidopyridin-3-yl)boronic acid, **55** and **56**) and subsequent *N*-Boc deprotection using TFA/CH_2Cl_2 provided compounds **48-53** (Scheme 8). In a similar manner, **43** was converted to **54**.

Scheme 8: Synthesis of compounds **48-54**.

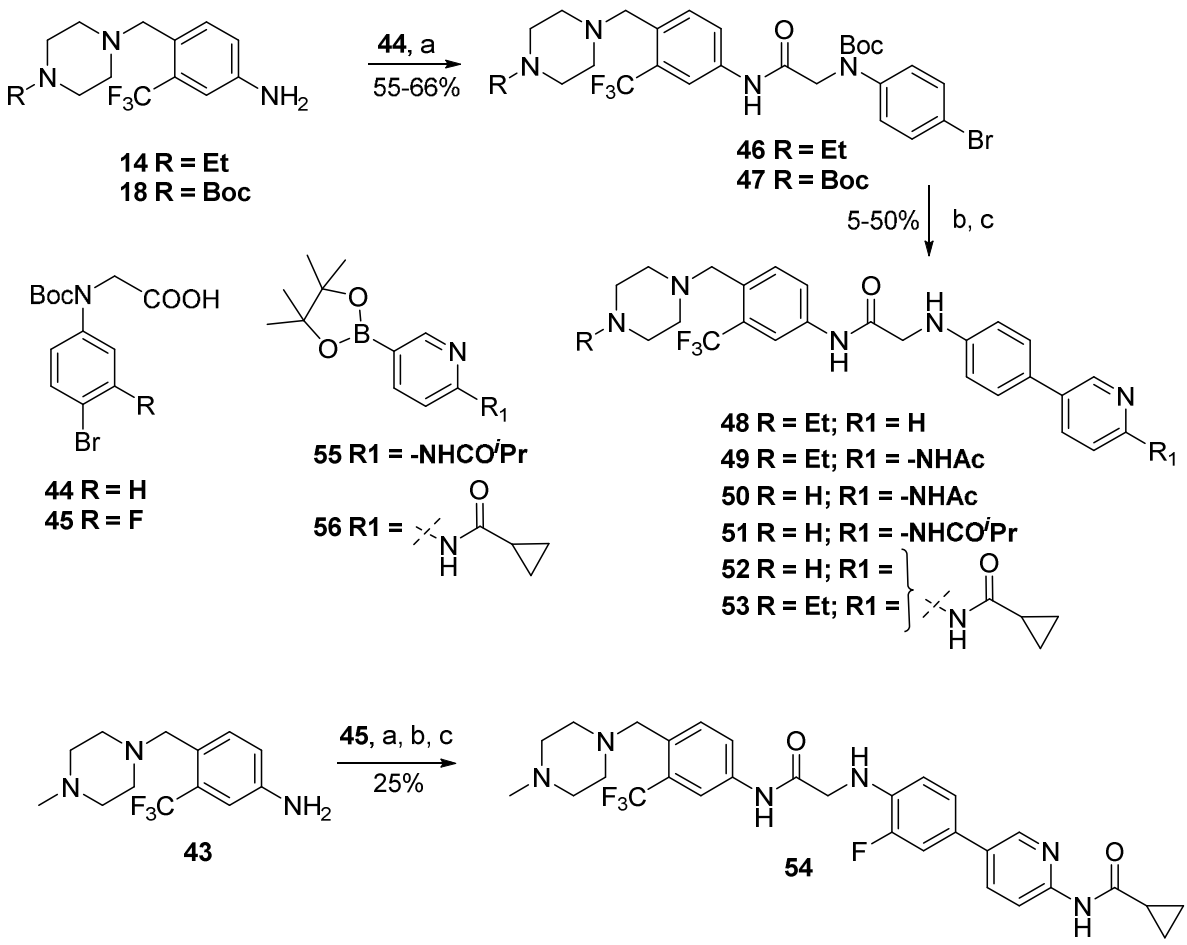

a) HATU, Et_3N, THF, rt; b) corresponding boronic acid or ester derivative (pyridine-3-boronic acid, (6-acetamidopyridin-3-yl)boronic acid, **55**, **56**), $Pd(dppfCl_2).CH_2Cl_2$, K_2CO_3, dioxane-water, 100 ^oC; c) TFA, CH_2Cl_2.

RESULTS AND DISCUSSION:

Compound **2** inhibits both MNK1 and MNK2 with IC_{50}'s of 1.76 μM and 20 nM, respectively (Table 1). In addition to MNK1 and MNK2, **2** inhibits several other kinases.[21] Our first objective was to improve the kinase selectivity profile of **2** while maintaining inhibition of MNK1 and MNK2. For this purpose, a brief SAR analysis was conducted. Modification of the urea linker to the corresponding amide derivatives **9** and **15** showed that this is tolerated in **15**, while **9** lost MNK1 inhibition and is >30 fold weaker on MNK2. Conversion of *N*-methylaminopyrimidine

Table 1. SAR of MNK1 and MNK2 inhibitors

ID	Structure	IC_{50} (μM)*		
		ABL1	MNK1	MNK2
2	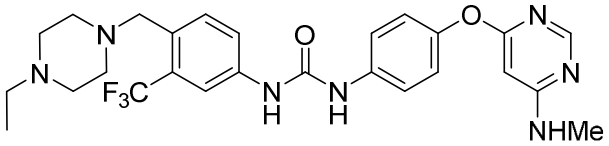	0.58	1.76	0.020
9	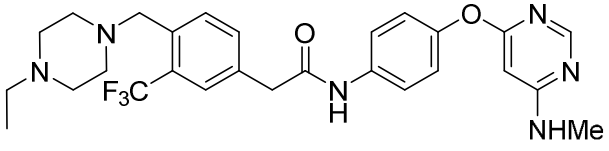	>10	>10	0.760
15	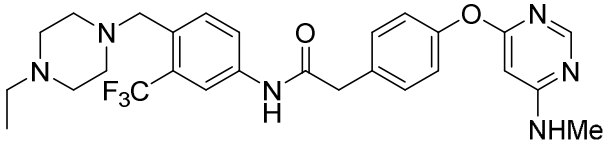	>10	3.69	0.022
16	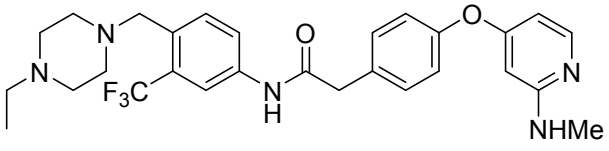	0.58	0.37	0.008
17	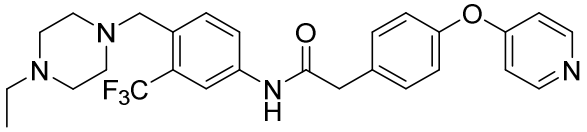	3.88	0.54	0.010
27	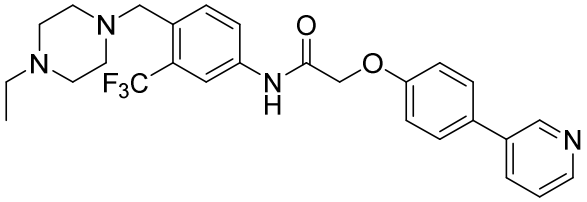	>10	0.57	0.014
48	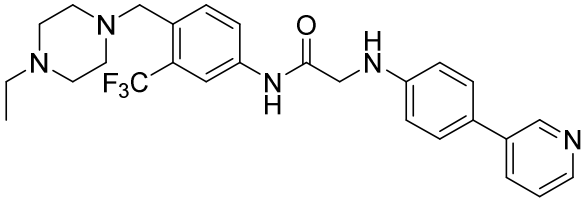	>10	0.35	0.011

**In vitro* IC_{50} against ABL1, MNK1 and MNK2; $n \geq 2$.

ring of **15** to *N*-methylpyridine-2-amine derivative **16** led to significant improvement in MNK1 inhibition. We also noticed that the *N*-methylamino group was not required for the inhibition of

MNK1 and 2 as indicated by IC_{50} values of **17**. Removal of biaryl ether oxygen and modification of phenylacetamide linker in **17** to a phenoxyacetamide for patentable structural novelty resulted in compound **27** which exhibited IC_{50}s of 577 nM and 14 nM against MNK1 & 2. The inhibitory profile of the corresponding amine analog **48** was similar to **27**. It may be noted that ABL1 inhibition was lost during these modifications. Apart from **16** with a donor-acceptor motif in the form of -*NH*-methylaminopyridine, none of the other compounds were able to show submicromolar inhibition of ABL1.

Any change to the position of nitrogen in the biaryl ring was not tolerated, as seen from the enzymatic activities of compounds **26** and **28** (Table 2).

Table 2. SAR of MNK1 and MNK2 inhibitors

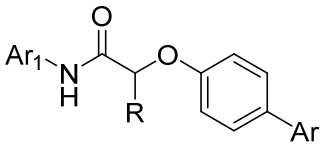

ID	Ar_1	R	Ar	IC_{50} (μM)*		
				ABL1	MNK1	MNK2
27	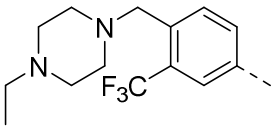	H	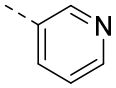	>10	0.57	0.014
26		H	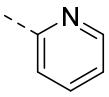	>10	>10	>10
28		H	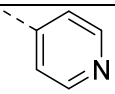	>10	>10	1.91
35	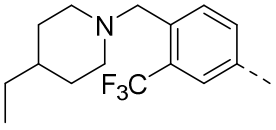	H	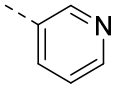	>10	4.51	0.082

38	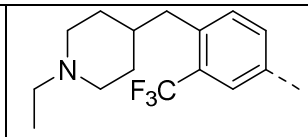	H	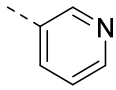	>10	>10	>10
40	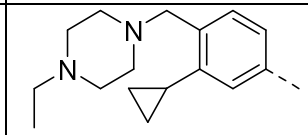	H	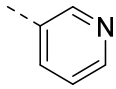	>10	>10	0.13
31	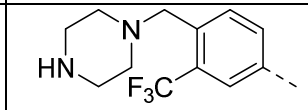	H	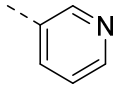	>10	0.35	0.012
42	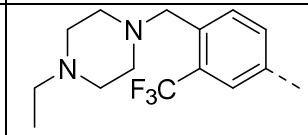	Me	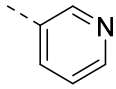	>10	>10	>10

**In vitro* IC_{50} against ABL1, MNK1 and MNK2; $n \geq 2$.

Presence of basic amines as in the piperazine motif was essential for MNK1 & 2 inhibition as shown by compounds **35** and **38**. While compound **35** showed weak MNK1 inhibition and more than 5 fold loss of MNK2 potency, **38** was inactive against both enzymes. We found that removal of *N*-ethyl group did not affect potencies against either enzyme. Replacement of $-CF_3$ with a cyclopropyl group resulted in loss of MNK1 potency with 10-fold weaker MNK2 inhibition. Introduction of a methyl group on the methylene carbon as in compound **42** also was not tolerated for MNK inhibition. Against ABL1, none of these compounds were active.

The kinase selectivity of **27** was evaluated at 1 μM using the KINOME*scan*™ approach (Ambit biosciences) against a panel of 104 kinases (Supporting Information Table S1). Profiling of compound **27** at 1 μM resulted in 90% inhibition of 11 kinases and showed a better selectivity index in comparison to **2**.

Molecular modeling of **27** with MNK2 and ABL1 enzyme models suggested the following interactions between the compound and protein (Figure 2): i) the protonated piperazine nitrogen may form a hydrogen bond in MNK2 with the carbonyl backbone of Ala202 and His203 (in

ABL1, the residues are Ile360 and His361); ii) -CF_3 group binds in a hydrophobic pocket in MNK2, formed by residues Leu133, Cys136, Val142, Leu196, Ile224 and Cys225 (in ABL1, Met290, Ile293, Leu298, Leu354, Val379 and Ala380); iii) nitrogen on the pyridine ring may form a hydrogen bond with the backbone nitrogen of MNK2 kinase hinge residue Met162 (Met318 in ABL1); iv) phenyl ring in the 5-position of the pyridine is sandwiched between the MNK2 gatekeeper Phe159 and Phe227 (in ABL1, gatekeeper Thr315 and Phe382); v) hydrogen bonding interaction between amide linker and the MNK2 backbone nitrogen of Glu129 (backbone nitrogen of Glu286 in ABL1). From these studies, we hypothesized that we could gain additional interaction with ABL1 protein by introducing substituents in the hinge binding region, and these modifications were suggested to be tolerated by both MNK1 and 2.

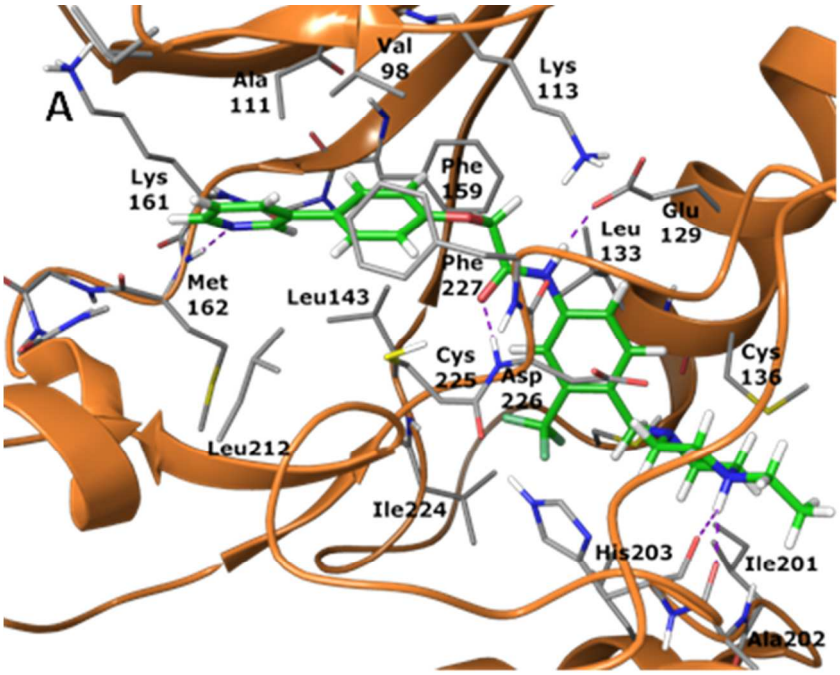

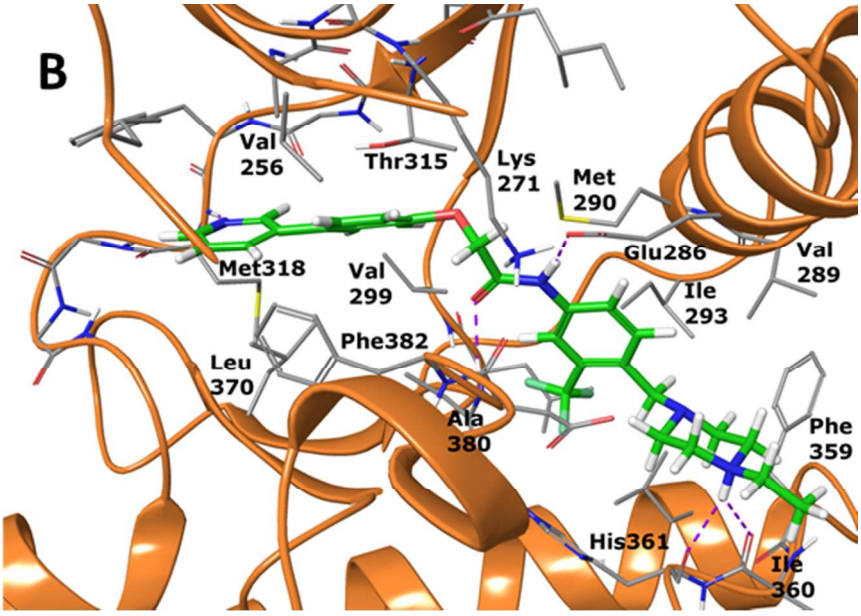

Figure 2: A) Compound **27** (stick representation; carbon in green, nitrogen in blue and oxygen in red) docked into the ATP-binding domain of: A) MNK2 (PDB entry 2AC3); B) ABL1 (PDB entry 3OXZ). The kinase domain is depicted as a cartoon with carbon atoms in gray, nitrogen in blue and oxygen in red.

Introduction of acetamide (**30**) resulted in 10-fold weaker inhibition of MNK1 while activity against MNK2 was maintained. Most importantly, **30** inhibited not only wild type ABL1, but also its T315I mutant with IC_{50}s 0.39 and 0.17 μM, respectively. The corresponding reverse amide derivative **29** exhibited complete loss of ABL1 and MNK1 inhibition with weak MNK2 inhibition. Compound **49**, the amine analog of **30**, showed similar activity profile as its ether analog. Removal of the *N*-Et group had little effect on its enzymatic and antiproliferative activity as shown by the data of compound **50**. Isopropyl amide analog **51** showed >10 μM inhibition of ABL1 with significant loss of MNK2 inhibition. Compound **52** with a cyclopropanamide moiety retained ABL1 and its T315I mutant inhibition while a 10-fold and 4-fold improvement was obtained in the inhibition of MNK1 & 2, respectively. This compound had good antiproliferative activity with a GI_{50} of 80 nM against K562 cells overexpressing eIF4E. Re-introducing the *N*-Et

moiety retained ABL1 and MNK2 inhibition while suffering a 5-fold loss over MNK1 inhibition with a GI_{50} of 51 nM in K562 cells overexpressing eIF4E as shown by compound **53**. Compound **54** with a fluorine on the phenyl ring improved ABL1 inhibition and MNK1 inhibition to 10 nM and 200 nM, respectively while retaining ABL1 T315I and MNK2 inhibition. **54** also exhibited very good antiproliferative activity as shown by its GI_{50} against K562 cells overexpressing eIF4E. In addition to the antiproliferative activity, these compounds also showed reduction in the phosphorylation of eIF4E at Ser209 in HeLa cells, with **50**, **53** and **54** as the most potent compounds in this assay.

Table 3. SAR of dual MNK1 & 2 and Abl inhibitors

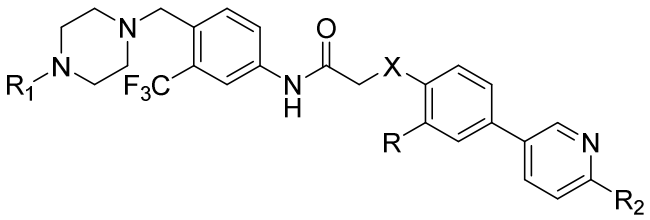

Comp-ound	R_1	X	R	R_2	IC_{50} (μM)^					GI_{50} (μM)
					ABL1 T315I	ABL1 native	MNK1	MNK2	HeLa*	K562 o/e eIF4E#
27	Et	O	H	H	ND	>10	0.57	0.014	0.098	>10
29	Et	O	H	-CONHMe	ND	>10	>10	6.86	ND	ND
30	Et	O	H	-NHAc	0.17	0.39	5.68	0.033	0.68	0.10
49	Et	NH	H	-NHAc	0.09	0.38	5.98	0.044	0.32	0.34
50	H	NH	H	-NHAc	0.24	0.88	3.92	0.032	0.20	0.40
51	H	NH	H	-NHCO^{i}Pr	>10	>10	7.70	0.13	0.86	3.30
52	H	NH	H	-NHCOCyc	0.10	0.21	0.51	0.008	0.32	0.08
53	Et	NH	H	-NHCOCyc	0.05	0.089	2.52	0.016	0.18	0.051

54	Me	NH	F	-NHCOCyc	0.02	0.01	0.20	0.010	0.28	0.012

^*In vitro* IC_{50} against ABL1, MNK1 and MNK2; $n \geq 2$. *concentration of the compound required for 50% reduction in the phosphorylation of eIF4E in HeLa cells; #concentration of the compound required for 50% reduction in the growth of K562 cells overexpressing eIF4E. The compounds were tested for dose response in triplicates. The dose response curve was done twice.

Docking studies suggested additional H-bonding interaction between the amide -NH and backbone carbonyl of the ABL1 hinge residue Met318 while the amide carbonyl may hydrogen bond to the –OH of the glycine-rich loop residue Tyr253 (Figure 3). While the reason behind the enhancement in the inhibition when a cyclopropyl group is introduced is not clear, additional interaction of this group with the neighboring residues Phe317, Thr319 and Leu248 in ABL1 may be a plausible explanation. The equivalent residues in MNK2 are Lys161, Arg163 and Leu90 (Figure 3).

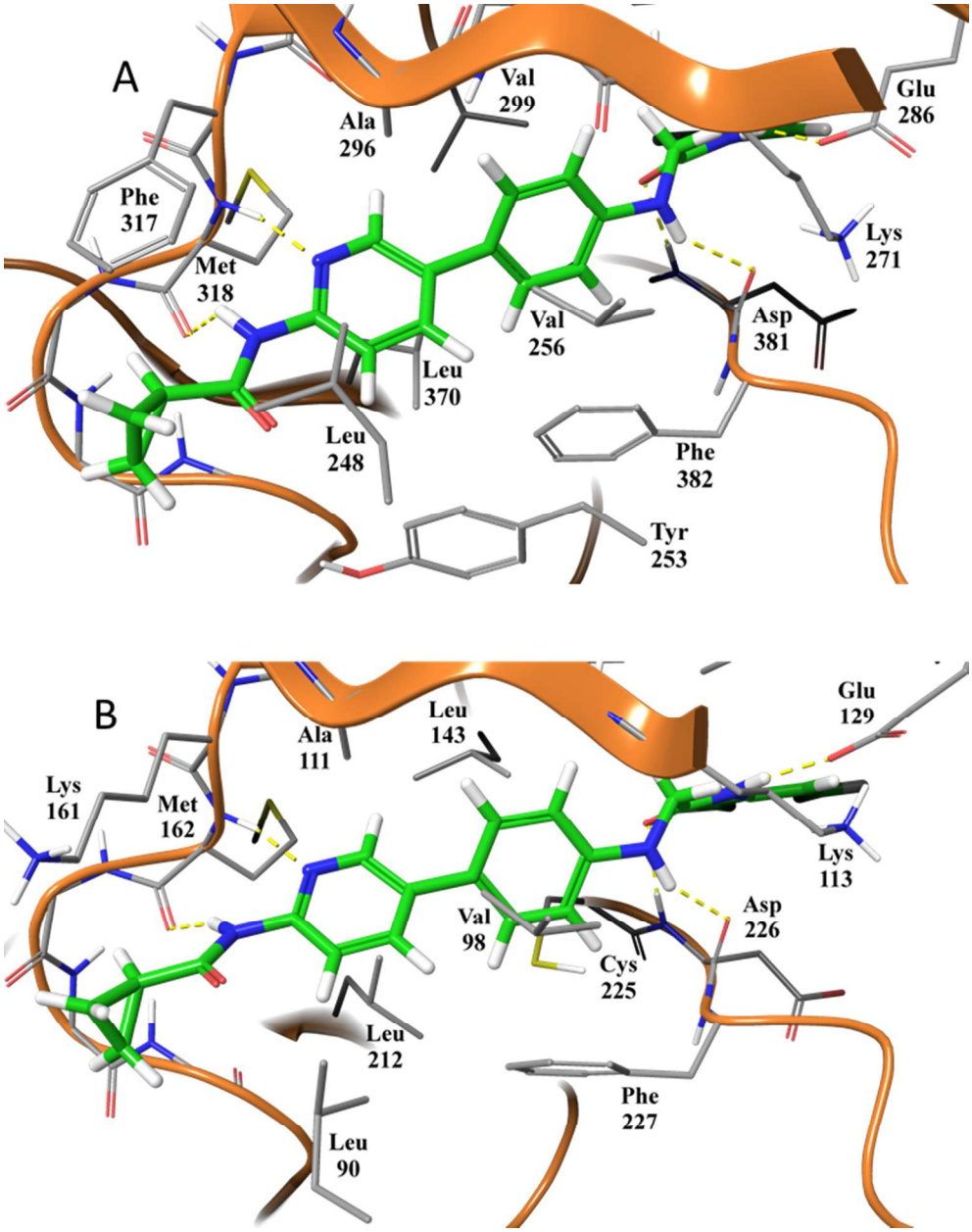

Figure 3: Compound **53** (tube representation; carbon in green, nitrogen in blue and oxygen in red) docked into the ATP-binding domain of: A) ABL1 (PDB entry 3OXZ); B) MNK2 (PDB entry 2AC3). The kinase domain is depicted as a cartoon with selected residues in thin tube with carbon atoms in gray, nitrogen in blue and oxygen in red.

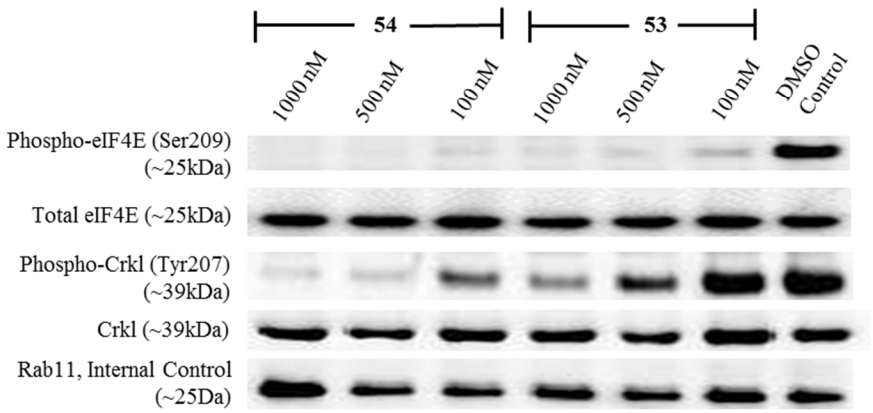

Figure 4: Inhibition of phosphorylation of eIF4E and Crkl by **53** and **54** in K562 cells overexpressing eIF4E. A) Total eIF4E and phospho-eIF4E (Ser209) were detected using anti-eIF4E and anti-phospho-eIF4E (Ser209) antibody; B) Crkl and phosphor-Crkl (Tyr207) were detected using anti-Crkl and anti-phospho-Crkl (Tyr207) antibody.

Figure 4 shows the ability of **53** and **54** to inhibit phosphorylation of both eIF4E (substrate of MNK1 & 2) and Crkl (substrate of ABL1) in K562 cells overexpressing eIF4E. Compound **54** inhibited phosphorylation of eIF4E at all tested concentrations with a dose dependent reduction of phosphor-Crkl, while **53** showed a dose dependent reduction of both phospho-eIF4E and phospho-Crkl. This is in agreement with the biochemical assay data with **54** being more potent inhibitor of both MNK1 & 2 and ABL1 than **53**.

Compounds **53** and **54** were tested in a panel of CML cell lines (Table 4). **54** showed potent anti-proliferative activity ranging from 1 nM to 13 nM while **53** was comparatively less potent with GI_{50} values of 15 nM to 58 nM across the 5 different CML cell lines. In comparison, imatinib exhibited values from 60 nM to 400 nM.

Table 4. Antiproliferative effect of **53** and **54** across a panel of CML cells

Compound	GI_{50} 48 h (μM)[#]				
	K562	BV-173	EM-2	KCL-22	JURL-MK1
53	0.058	0.030	0.015	0.050	0.030
54	0.012	0.001	0.001	0.013	0.001
Imatinib	0.200	0.10	0.26	0.43	0.06

[#]The compounds were tested for dose response in triplicate. The dose response curve was done twice.

Selectivity screen of **53** and **54** in the kinase panel (104 kinases, Ambit KINOME*scan*™) showed that at 1 μM, these compounds inhibited 90% activity of 12 and 15 kinases, respectively (supporting information Table S1). Biochemical IC_{50}s were determined for those kinases against which both compounds showed >99% inhibition (table 5). Among these, RET was most potently inhibited by **53** and **54** followed by FLT3 and VEGFR2 with IC_{50}s $\leq$ 24 nM while showing comparatively weaker inhibition of KIT, PDGFRα, PDGFRβ and FGFR2.

Table 5: IC_{50} of **53** and **54** against selected kinases.

Kinase	IC_{50} (μM)*	
	53	**54**
FLT3	0.020	0.020
VEGFR2	0.024	0.021
RET	0.007	0.001
cKIT	0.888	1.509
FGFR2	0.930	0.272
PDGFRα	0.672	1.280

PDGFRβ	1.083	1.055

*Inhibition of kinase activity, n=2.

In general, thermodynamic solubility of compounds in the series was low at pH 7, with **53** and **54** exhibiting 127.5 and 182.7 µg/mL, respectively at pH 4 (Table 6). Both these compounds did not inhibit CYP3A4 and CYP2D6. Compounds **53** and **54** also showed high plasma protein binding (Table 6). *In vivo* pharmacokinetic studies of **53** and **54** showed oral bioavailability of 80 and 31 %, respectively (Table 7).

Table 6. *In vitro* PK parameters and thermodynamic solubility of selected compounds

Compound	CYP IC_{50} (µM)		PAMPA (10^{-6} cm/s)	Human PPB (%)	Thermodynamic solubility (µg/mL)	
	3A4	2D6			pH 7	pH 4
49	3.2	>20	26.2	ND	0.6	ND
50	2.4	>20	1.13	ND	ND	131.5
52	1.1	>20	5.53	ND	ND	109.1
53	>30	>30	34.53	99.92	0.1	127.5
54	>30	>30	30.61	99.78	3.8	182.7

ND – Not Determined.

Table 7: *In vivo* PK properties of **53** and **54** in CD-1 mice

Compound	iv[a]		po 50 mg/kg[b]		F (%)
	Cl (L/h/kg)	$T_{1/2}$ (h)	C_{max} (ng/ml)	AUC (ng.h/ml)	
53	2.7	2.14	2490	14337	80
54	3	2.2	1212	5128	31

[a]formulated in 50% PEG+sterile MQ water as clear solution. **53** and **54** were dosed at 5 and 10 mg/kg respectively; [b]formulated in 0.5% methylcellulose + 0.1% Tween 80 + sterile MQ water as suspension. See supporting information table S4 for full pharmacokinetic parameters.

In an *in vivo* xenograft model employing K562 cells overexpressing eIF4E in NOD-SCID mice, both **53** and **54** inhibited tumor growth in a dose-dependent manner when dosed orally, QD for 14 days (Figure 5). Complete tumor regression was observed at 100 mg/kg for **54** while **53** showed dose dependent tumor growth inhibition at 100 and 200 mg/kg. Importantly, mice given **53** and **54** at these doses did not exhibit toxicity. Imatinib at 200 mg/kg QD resulted in 57% tumor growth inhibition. We also monitored phosphorylation of eIF4E in the tumor tissues after compound administration on day 14 (Figure 6). For both **53** and **54** at 50 mg/kg, maximum inhibition of phosphorylation of eIF4E in the tumor was seen after 4 h of drug administration. Thus, inhibition of BCR-ABL1 kinase activity resulted in tumor size shrinkage while its MNK1 and MNK2 inhibition prevented phosphorylation of eIF4E *in vivo*. A 10-fold better inhibition of MNK1 by **54** is reflected in greater inhibition of phosphorylation of eIF4E in tumor tissues in comparison to **53**. The difference in tumor growth inhibition of these two compounds in the mouse xenograft model could be attributed to enhanced Abl inhibition of **54** over **53**.

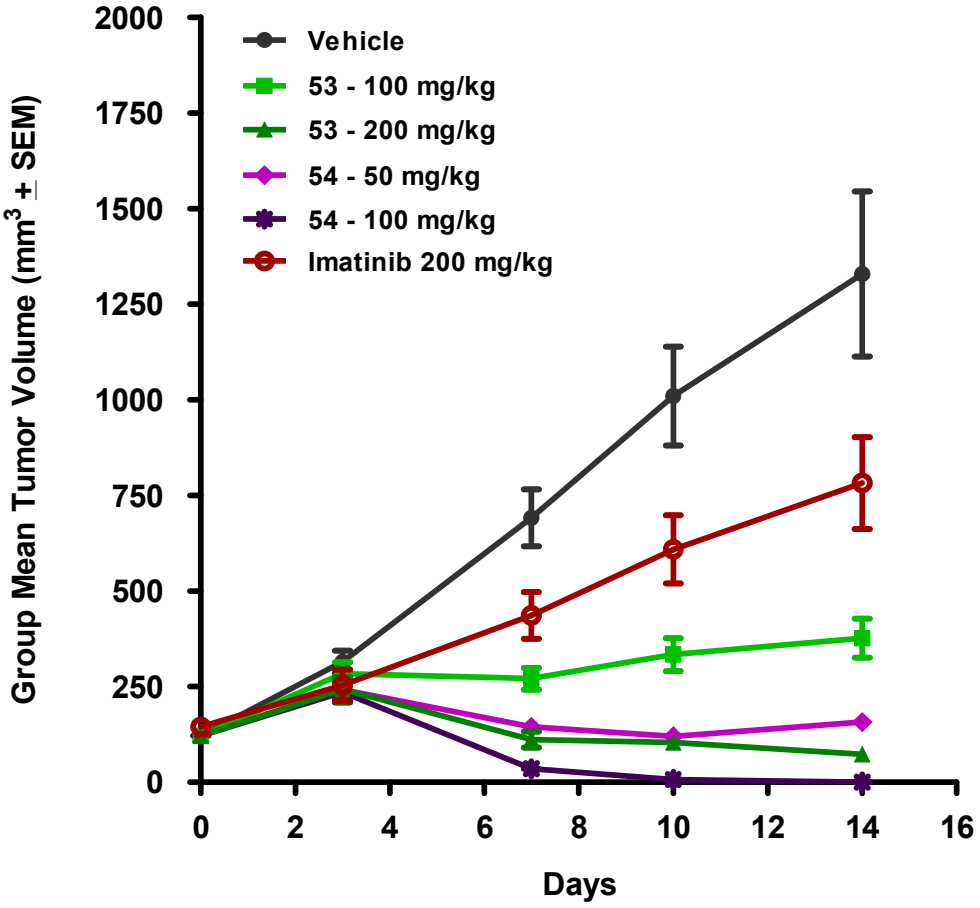

Figure 5: Mouse efficacy study of **53** and **54** in a K562 o/e eIF4E xenograft model. Compounds **53**, **54** and imatinib were administered by oral gavage, single dose per day for 14 days. Compound **53** showed a dose dependent tumor growth inhibition at 100 and 200 mg/kg while **54** showed complete tumor regression at 100 mg/kg.

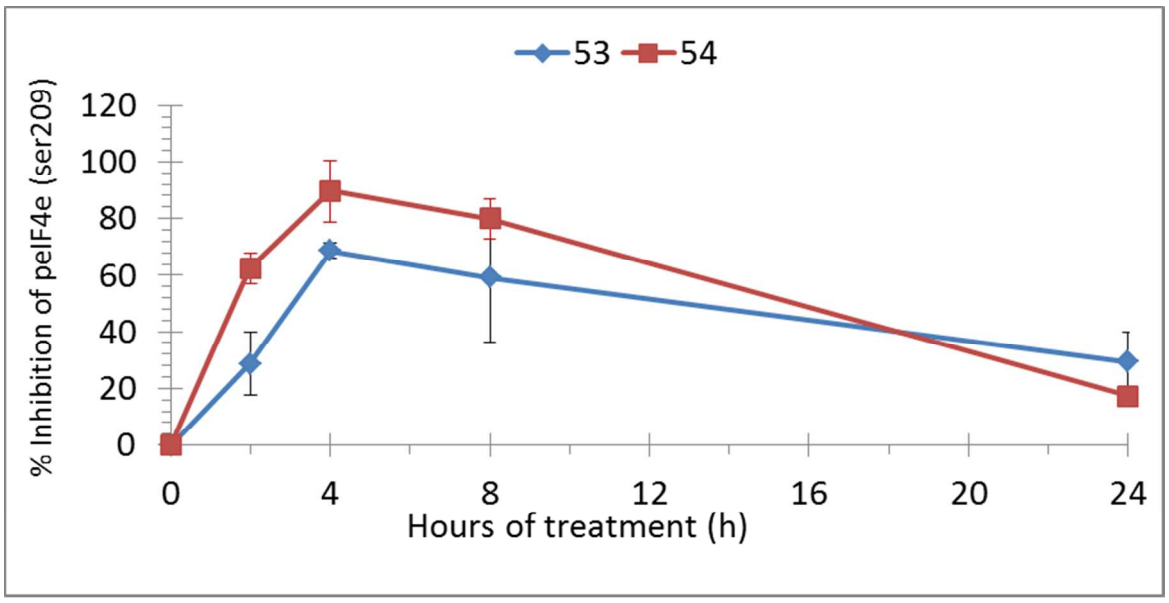

Figure 6: Inhibition of phosphorylation of eIF4E by **53** and **54** in tumor tissue samples after 14 day QD study. Maximum inhibition was observed at 4 hours after compound administration.

The effect of these compounds on the self-renewal capacity of hematopoietic stem cells and patient derived BC CML samples (primary $CD34^+$ cells) *ex vivo* was further evaluated (Sharon Lim *et al*, unpublished results).[28,29] Results of these experiments and detailed biological characterization of these compounds will be published in due course.

Conclusion

We have identified novel inhibitors of MNK1, MNK2 and BCR-ABL1 which are orally available and capable of effective target engagement *in vivo*. While BCR-ABL1 inhibition brings potent antiproliferative activity against CML cells, MNK1 & 2 inhibition prevents eIF4E phosphorylation which is known to prevent self-renewal capacity of LSCs.[6] As current CML therapy using tyrosine kinase inhibitors do not eliminate LSCs, dual Abl-MNK1 & 2 inhibitors such as **53** and **54** might be beneficial in treating patients with CML and may warrant further studies to evaluate their usefulness as clinical agents.

Experimental Section:

Molecular modeling: The MNK2 X-ray structure PDB entry 2AC3[30] and ABL1 X-ray structure PDB entry 3OXZ[31] was downloaded from the Protein Data Bank [www.pdb.org] and prepared with the protein preparation wizard in Maestro 9.3 (Schrödinger, LLC, New York, NY, USA, 2012) using standard settings. This included the addition of hydrogen atoms, bond assignments, removal of water molecules further than 7Å from the ligand, protonation state assignment, optimization of the hydrogen bond network and restrained minimization using the OPLS2005 force field.[32] The prepared ABL1 structure was used as is where as a model was built of the MNK2 activation loop using the prepared ABL1 structure as a template. The Mnk2 structure was superimposed on ABL1 using the protein structural alignment tool in Maestro. The activation loop residues 226-231 in MNK2 were manually modeled to have the same backbone torsions as found in the ABL1 structure. The sidechains of these residues was modeled as homologous ABL1 residues except Asp228 which is a glycine in ABL1. The Asp228 sidechain was positioned to form a salt bridge to Lys113.

The inhibitors were build using Maestro and minimized to conversion using the OPLS2005 force field and GB/SA continuum solvation method[33] as implemented in Macromodel 9.9 (Schrödinger, LLC, New York, NY, USA, 2012). The inhibitors were then manually docked into the ABL1 and MNK2 binding site using the ABL1 co-crystalized ligand ponatinib as a template for the bioactive conformation and binding orientation. The inhibitor-protein complex was finally minimized using Macromodel. All residues more than 7Å from the ligand were constrained before the complex was subjected to 500 steps of Polak-Ribiere-Conjugate-Gradient[34] minimization using the OPLS2005 force field and GB/SA continuum solvation method.[33] The PDB files of compounds **27** and **53** modeled into MNK2 are available in Supporting Materials.

General Procedures. All reagents were purchased from commercial sources and used as received. Reaction progress was monitored by TLC using Merck silica gel 60 F254 on glass plates with detection by UV at 254 nM. LC−MS analysis was carried out with a Shimadzu LC-20AD and LCMS-2020. The column used was a Phenomenex Kinetex 2.6 μm, 50 × 2.10 mm). Proton and ^{13}C nuclear magnetic resonance (^{1}H and ^{13}C NMR) spectra were obtained using a Bruker Ultrashield 400 PLUS/R system, operating at 400 MHz and 100 MHz respectively. All resonance bands were referenced to tetramethylsilane (internal standard). Splitting patterns are indicated as follows: s, singlet; d, doublet; t, triplet; m, multiplet; br, broad peak. The compound purities were >95%, determined by Varian Prostar HPLC instrument (column: Phenomenex kinetex 2.6 μm XB-C18A 100A, 50 x 4.6 mm; solvent A: H_2O/0.1% HCO_2H; solvent B: MeCN/0.1% HCO_2H; run time 10.5 min.; time/%B: 0.0/10, 2.0/10, 7.5/90, 9.0/90,10.0/10, 10.5/10; flow rate: 2 mL/min.; wavelength: 254 nm). Melting points were determined in Pyrex capillary tubes using a StuartnSMP30 melting point apparatus. Purification of final compounds and intermediates was carried out via normal or reverse phase chromatography. Normal-phase chromatography was performed on an ISCO CombiFlash system with either an ISCO RediSep or a Biotage silica gel disposable column eluted with EtOAc/hexanes or methanol/CH_2Cl_2. Reverse-phase chromatography was performed on a Shimadzu preparative system on a Phenomenex Luna or Sunfire C18 preparative column with appropriate gradients of MeCN/H_2O/0.1% trifluoroacetic acid (TFA) or methanol/H_2O/0.1% TFA as eluent at a flow rate of 40 mL/min.

(4-((4-Ethylpiperazin-1-yl)methyl)-3-(trifluoromethyl)phenyl)methanol (6): To a stirred suspension of $LiAlH_4$ (0.17 g, 4.53 mmol) in THF (25 mL) was added **5** (1.0 g, 3.02 mmol) in THF (5 mL) at 0 ^{o}C. After 4 h at room temperature, the reaction mixture was quenched (sat. aq. Na_2SO_4) at 0 ^{o}C, filtered through celite pad and concentrated. The residue was partitioned

between EtOAc and water. The organic layer was separated, dried (anh. Na_2SO_4), evaporated and the residue purified by silica gel column chromatography (100–200 mesh) using 30% EtOAc in hexane as eluent to afford **6** (0.65 g, 71%). ^{1}HNMR ($CDCl_3$): δ 7.78-7.76 (d, *J* = 8.0 Hz, 1H), 7.63 (s, 1H), 7.52-7.50 (d, *J* = 8.0 Hz, 1H), 4.73 (s, 2H), 3.65 (s, 2H), 2.51-2.39 (m, 10H), 1.10-1.06 (t, *J* = 7.2 Hz, 3H). LCMS (ESI) *m/z* 303.2 $(M+H)^+$.

2-(4-((4-Ethylpiperazin-1-yl)methyl)-3-(trifluoromethyl)phenyl)acetic acid (7): To a solution of **6** (0.65 g, 2.15 mmol) in CH_2Cl_2 (10 mL) was added Et_3N (0.66 g, 6.6 mmol) and MsCl (0.41 g, 3.63 mmol) at 0 °C. After stirring at room temperature for 16 h, the reaction mixture was diluted with CH_2Cl_2 and washed with water. The organic layer was dried, evaporated and the crude residue (0.5 g, 1.56 mmol) redissolved in DMSO (5 mL). NaCN (0.15 g, 3.12 mmol) in water (0.5 mL) was added and the reaction mixture was heated at 90 °C for 14 h. The reaction mixture was cooled to 0 ^{o}C, water (15 mL) was added and extracted with EtOAc (3x5 mL). The organic layer was washed with water (1x5 mL), brine (1x5 mL), dried over anhydrous Na_2SO_4 and evaporated. The residue was purified by column chromatography over silica gel (100–200 mesh) using a solvent gradient of 1% MeOH in CH_2Cl_2 as eluent to afford 0.14 g of 2-(4-((4-ethylpiperazin-1-yl)methyl)-3-(trifluoromethyl)phenyl)acetonitrile [^{1}H NMR: (DMSO-d_6): δ 1.08-1.12 (t, *J* = 7.0 Hz, 3H), 2.48-3.33 (m, 10H), 3.66 (s, 2H), 3.78 (s, 2H), 7.61-7.59 (d, *J* = 8.0 Hz, 1H), 7.67 (s, 1H), 7.78 (d, *J* = 8.0 Hz, 1H)] which was treated with 6N HCl (5 mL) at 90 ^{o}C for 16 h. The reaction mixture was evaporated, the residue dissolved in methanol (1 mL) and triturated with Et_2O at 0 °C. The solid formed was filtered and dried to afford (0.10 g, 14 % over 3 steps) of **7** as hydrochloride salt. ^{1}H NMR (DMSO-d_6): δ 7.83-7.85 (d, *J* = 8.0 Hz, 1H), 7.57 (s, 1H), 7.49-7.51 (d, *J* = 8.0 Hz, 1H), 3.89 (s, 2H), 3.73 (s, 2H), 3.67-3.49 (m,

2H), 3.17-3.08 (m, 6H), 2.68-2.60 (m, 2H), 1.25-1.23 (t, J = 6.0 Hz, 3H). LCMS (ESI) *m/z* 331.2 $(M+H)^+$.

2-(4-((4-Ethylpiperazin-1-yl)methyl)-3-(trifluoromethyl)phenyl)-*N*-(4-((6-(methylamino)-pyrimidin-4-yl)oxy)phenyl)acetamide (**9**): **7** (0.1 g, 0.30 mmol) and **8** (0.06 g, 0.30 mmol) were dissolved in 3 mL of anhydrous DMF. HBTU (0.138 g, 0.36 mmol) and Et_3N (0.10 mL, 0.72 mmol) were subsequently added and the resulting reaction mixture was stirred for 16 h, diluted with water (30 mL) and extracted with EtOAc (3x15 mL). The combined organic layers were washed with brine, dried over sodium sulfate and evaporated under reduced pressure. The residue was purified by preparative HPLC to afford **9** (10.6 mg, 6 % yield) as a solid. ^{1}HNMR (DMSO-d_6): δ 10.27 (s, 1H), 8.11 (s, 1H), 7.69-7.71 (m, 1H), 7.67 (s, 1H), 7.58-7.62 (m, 3H), 7.24-7.25 (m, 1H), 7.05-7.08 (m, 2H), 5.71 (s, 1H), 3.74 (s, 2H), 3.57 (s, 2H), 2.75 (s, 3H), 2.29-2.38 (m, 10H), 0.96-0.99 (t, J = 7.2 Hz, 3H); ^{13}C NMR (DMSO-d_6): δ 168.4, 165.1, 148.1, 135.9, 135.5, 135.1, 133.0, 130.5, 127.1- 126.2 (q), 125.7, 123.0, 121.6, 120.2, 57.4, 52.7, 52.2, 51.4, 42.2, 27.3, 11.8. LCMS (ESI) *m/z* 529 $(M+H)^+$. HPLC purity: 99.3%; retention time: 3.85 min.; Melting point: 147.9 ^{o}C.

2-(4-((2-Chloropyridin-4-yl)oxy)phenyl)acetic acid (**11**): To a solution of **10** (2.45 g, 14.7 mmol) and 2,4-dichloropyridine (2.18 g, 14.7 mmol) in 8 mL of DMF was added K_2CO_3 (3.05 g, 22.1 mmol). After 16 h at 90 ^{o}C, the reaction mixture was cooled to room temperature, diluted with water (80 mL) and extracted with EtOAc (3x25 mL). The combined organic layer was washed with brine, dried over sodium sulfate and evaporated under reduced pressure. The residue was purified by flash column chromatography eluting with 1:4 EtOAc:hexane to yield 1.68 g of methyl 2-(4-((2-chloropyridin-4-yl)oxy)phenyl)acetate as a pale yellow oil [^{1}HNMR ($CDCl_3$): δ 8.22 (s, 1H), 7.35-7.37 (d, J = 8.0 Hz, 1H), 7.12-7.14 (d, J = 8.8 Hz, 2H), 7.05-7.07

(d, J = 8.0 Hz, 1H), 6.81-6.83 (d, J = 8.8 Hz, 2H), 3.69 (s, 3H), 3.55 (s, 2H); LCMS (ESI) *m/z* 278 $(M+H)^+$] which was dissolved in THF containing water (25 mL, 1:1) and treated with LiOH (0.220 mg, 9.09 mmol). After 14 h, the reaction mixture was acidified with aq. citric acid. The solid formed was filtered, washed with water and dried *in vacuuo* to afford 1.59 g (40 % over two steps) of **11**. ^{1}H NMR ($CDCl_3$): δ 8.23 (d, J = 5.7 Hz, 1H), 7.39-7.37 (m, 2H), 7.08-7.06 (m, 2H), 6.84-6.83 (m, 1H), 6.81-6.79 (m, 1H), 3.71 (s, 2H); LCMS (ESI) *m/z* 264.1 $(M+H)^+$.

2-(4-((2-(Methylamino)pyridin-4-yl)oxy)phenyl)acetic acid (**13**)**:** A solution of **12** (200 mg, 0.75 mmol) in THF (15 mL) was treated with aq.$MeNH_2$ (15 mL) at 80 °C. After 15 h, the reaction mixture was cooled to room temperature, evaporated and the residue purified by preparative HPLC to afford 101 mg (54%) of **13** as a white solid. ^{1}H NMR (DMSO-d_6): δ 12.40 (brs, 1H), 8.31 (brs, 1H), 7.90-7.92 (d, J = 8.0 Hz, 1H), 7.40-7.43 (d, J = 8.5 Hz, 2H), 7.20-7.17 (d, J = 8.5 Hz, 2H), 6.58 (m, 1H), 6.10 (s, 1H), 3.64 (s, 2H), 2.83-2.85 (m, 3H); LCMS (ESI) *m/z* 259.2 $(M+H)^+$.

***N*-(4-((4-Ethylpiperazin-1-yl)methyl)-3-(trifluoromethyl)phenyl)-2-(4-((6-(methylamino)-pyrimidin-4-yl)oxy)phenyl)acetamide** (**15**): To a solution of **12** (0.10 g, 0.38 mmol) and **14** (0.11 g, 0.38 mmol) in DMF (4 mL) of was added HATU (174 mg, 0.45 mmol) and Et_3N (0.06 mL, 0.45 mmol). After stirring at room temperature for 3 h, the reaction mixture was diluted with water and extracted with EtOAc (3x10 mL). The combined organic extracts were washed with brine, dried over sodium sulfate and evaporated under reduced pressure and the residue purified by flash column chromatography, eluting with MeOH:CH_2Cl_2 (1:20) to afford 151 mg of 2-(4-((6-chloropyrimidin-4-yl)oxy)phenyl)-*N*-(4-((4-ethylpiperazin-1-yl)methyl)-3-(trifluoromethyl)-phenyl)acetamide [LCMS (ESI) *m/z* 534 $(M+H)^+$] which was dissolved in THF and treated with $MeNH_2$ (3 mL of 2.0 M solution in THF) in a sealed tube. After heating at 80 ^{o}C for 16 h, the

reaction mixture was evaporated and the residue purified *via* preparative HPLC eluting with 10%-40% of MeCN in water containing 0.1% formic acid. The fractions containing the compound were evaporated and the residue partitioned between CH_2Cl_2 and sat. $NaHCO_3$ solution. The organic layer was washed with brine, dried over sodium sulfate and evaporated under reduced pressure to yield **15** (49.1 mg, 25% over two steps) as a solid. ^{1}HNMR (DMSO-d_6): δ 10.47 (s, 1H), 8.11 (s, 1H), 8.05 (s, 1H), 7.77-7.79 (m, 1H), 7.64-7.66 (m, 1H), 7.35-7.37 (d, J = 6.8 Hz, 2H), 7.26-7.28 (m, 1H), 7.07-7.08 (d, J = 6.8 Hz, 2H), 5.77 (s, 1H), 3.66 (s, 2H), 3.52 (s, 2H), 3.29 (s, 3H), 2.29-2.49 (m, 10H), 0.95-0.97 (t, J = 7.2 Hz, 3H); ^{13}C NMR (DMSO-d_6): δ 169.4, 165.0, 157.8, 151.5, 138.0, 132.2, 131.5, 131.2, 130.2, 128.2-126.9 (q), 125.5, 122.8, 122.2, 121.2, 120.0, 115.9, 115.8, 57.3, 52.6, 52.2, 51.4, 42.4, 27.3, 11.8. LCMS (ESI) *m/z* 529 $(M+H)^+$. HPLC purity: 99.6%; retention time: 3.93 min. Melting point: 85.5 ^oC.

***N*-(4-((4-Ethylpiperazin-1-yl)methyl)-3-(trifluoromethyl)phenyl)-2-(4-((2-(methylamino)-pyridin-4-yl)oxy)phenyl)acetamide** (**16**): To a solution of **13** (0.05 g, 0.19 mmol) and **14** (0.055 g, 0.19 mmol) in anhydrous DMF (2 mL), was added HATU (0.148 g, 0.38 mmol) and Et_3N (0.05 mL, 0.38 mmol). After stirring at room temperature for 1.5 h, the reaction mixture was diluted with water and extracted with EtOAc (3 x 10 mL). The combined organic extracts were washed with brine, dried over sodium sulfate and evaporated under reduced pressure and the residue purified by preparative HPLC eluting with 10%-40%-95% of MeCN containing 0.1% formic acid over 55 minutes. The fractions containing the compound were evaporated and the residue partitioned between CH_2Cl_2 and sat. aq. $NaHCO_3$ solution. The organic layer was washed with brine, dried over sodium sulfate and evaporated under reduced pressure to yield **16** (33.9 mg, 33 % yield) as a white solid. ^{1}HNMR (DMSO-d_6): δ 10.48 (s, 1H), 8.06-8.05 (d, J = 2.0 Hz, 1H), 7.87-7.86 (d, 1H), 7.79-7.77 (d, J = 8.4 Hz, 1H), 7.67-7.65 (d, J = 8.4 Hz, 1H), 7.40-7.38 (d,

J = 8.2 Hz, 2H), 7.09-7.07 (d, *J* = 8.2 Hz, 2H), 6.46-6.44 (m, 1H), 6.12-6.10 (dd, *J* = 5.6, 1.6 Hz, 1H), 5.83-5.82 (d, *J* = 2.0 Hz, 1H), 3.67 (s, 2H), 3.52 (s, 2H), 2.70-2.69 (m, 3H), 2.37-2.27 (m, 10H), 0.99-0.95 (t, *J* = 6.8 Hz, 3H); ^{13}C NMR (DMSO-d_6): δ 169.3, 164.7, 161.2, 152.7, 149.3, 138.0, 132.1, 131.5, 131.2, 130.7, 128.2, 127.7-0 (q), 125.5, 122.8, 122.2, 120.3, 115.9, 115.8, 101.8, 93.4, 57.3, 52.6, 52.2, 51.4, 42.3, 27.9, 11.8. LCMS (ESI) *m/z* 528 $(M+H)^+$. HPLC purity: 100%; retention time: 3.53 min. Melting point: 59.9 ^{o}C.

***N*-(4-((4-Ethylpiperazin-1-yl)methyl)-3-(trifluoromethyl)phenyl)-2-(4-(pyridin-4-yloxy)-phenyl)acetamide (17): 11** (0.32 g, 1.21 mmol) was dissolved in EtOH (10 mL) and hydrogenated over Pd/C using Thalesnano H-cube for 2 cycles at full H_2 mode at 30 ^{o}C and 0 bar. The resulting solution was evaporated under reduced pressure to yield 2-(4-(pyridin-4-yloxy)phenyl)acetic acid [0.282 g, 1.23 mmol, LCMS: (ESI) *m/z* 230 $(M+H)^+$] which was re-dissolved in DMF (3 mL) containing **14** (0.353 mg, 1.23 mmol), HATU (0.935mg, 2.46 mmol) and Et_3N (0.35 mL, 2.46 mmol). After stirring at room temperature for 30 minutes, the reaction mixture was diluted with water and extracted with EtOAc (3x10 mL). The combined organic extracts were washed with brine, dried over sodium sulfate and evaporated under reduced pressure. The residue was purified by preparative HPLC, eluting with 15%-50%-95% of MeCN containing 0.1% formic acid. The fractions containing the compound were evaporated and the residue partitioned between CH_2Cl_2 and sat. $NaHCO_3$ solution. The organic layer was washed with brine, dried over sodium sulfate and evaporated under reduced pressure to yield **17** (100 mg, 16 % over two steps) as a gum. ^{1}HNMR (DMSO-d_6): δ 10.47 (s, 1H), 8.45-8.40 (m, 2H), 8.06 (d, *J* = 1.7 Hz, 1H), 7.78 (d, *J* = 8.4 Hz, 1H), 7.66 (d, *J* = 8.4 Hz, 1H), 7.43 (d, *J* = 8.5 Hz, 2H), 7.14 (d, *J* = 8.5 Hz, 2H), 6.91-6.89 (m, 2H), 3.70 (s, 2H), 3.52 (s, 2H), 2.36-2.27 (m, 10H), 0.97 (t, *J* = 7.2 Hz, 3H); ^{13}C NMR (DMSO-d_6): δ 169.3, 163.9, 152.2, 151.3, 138.0, 132.7, 131.5,

131.2, 131.0, 128.2, 127.8-126.9 (q), 125.5, 122.8, 122.2, 120.4, 115.9, 115.8, 111.8, 57.3, 52.6, 52.2, 51.4, 42.3, 11.8. LCMS (ESI) *m/z* 499 $(M+H)^+$. HPLC purity: 99.7%; retention time: 3.11 min.

2-(4-Bromophenoxy)-*N*-(4-((4-ethylpiperazin-1-yl)methyl)-3-(trifluoromethyl)phenyl)-acetamide (**24**): To a solution of **19** (1.20 g, 4.66 mmol) in anhydrous CH_2Cl_2 (10 mL) was added oxalyl chloride (0.59 g, 4.66 mmol) followed by a few drops of DMF at 0 ^oC. After stirring at room temperature for 1 h, a solution of **14** (2.50 g, 8.69 mmol) and Et_3N (1.84 mL, 26.0 mmol) in anhydrous CH_2Cl_2 (10 mL) was added dropwise at 0 ^oC and warmed to room temperature. After 16 h, the reaction mixture was partitioned between water (200 mL) and dichloromethane (100 mL). The organic layer was washed with brine (400 mL), dried (Na_2SO_4), the solvent evaporated and the residue purified by flash chromatography (Redisep silica gel, 97:3 CH_2Cl_2/MeOH) to afford **24** (2.2 g, 80%) as a solid. ^1H NMR (DMSO-d_6): δ 10.37 (s, 1H), 8.06 (s, 1H), 7.85-7.83 (dd, *J* = 8.4, 1.7 Hz, 1H), 7.69-7.66 (d, *J* = 8.4 Hz, 1H), 7.49-7.47 (d, *J* = 8.8 Hz, 2H), 6.99-6.97 (d, *J* = 8.8 Hz, 2H), 4.72 (s, 2H), 3.53 (s, 2H), 2.37-2.27 (m, 10H), 0.99-0.95 (t, *J* = 7.2 Hz, 3H); LCMS (ESI) *m/z* 499 $(M+H)^+$.

***Tert*-butyl 4-(4-(2-(4-bromophenoxy)acetamido)-2-(trifluoromethyl)benzyl)piperazine-1-carboxylate** (**25**): Synthesized in 50% yield using **18** and **19** following the method of synthesis of **24** as a colorless oil. ^1H NMR ($CDCl_3$): δ 8.27 (s, 1H), 8.06 (s, 1H), 7.80-7.78 (m, 2H), 7.47-7.45 (d, *J* = 4.8 Hz, 2H), 7.47-7.45 (d, *J* = 4.8 Hz, 2H), 4.60 (s, 2H), 3.62 (s, 2H), 3.44-3.41 (m, 4H), 2.40-2.39 (m, 4H), 1.45 (s, 9H); LCMS (ESI) *m/z* 572.2 $(M+H)^+$.

***N*-(4-((4-Ethylpiperazin-1-yl)methyl)-3-(trifluoromethyl)phenyl)-2-(4-(pyridin-2-yl)-phenoxy)acetamide** (**26**): Synthesized as described in the procedure for **9** using **14** and **20** in

67% yield as a white solid. ^{1}H NMR (DMSO-d_6): δ 10.43 (s, 1H), 8.62–8.61 (m, 1H), 8.09 (s, 1H), 8.07–8.05 (d, J = 8.8 Hz, 2H), 7.93–7.83 (m, 3H), 7.69–7.67 (d, J = 8.8 Hz, 1H), 7.30–7.27 (m, 1H), 7.12–7.10 (d, J = 8.8 Hz, 2H), 4.80 (s, 2H), 3.48–2.91 (m, 10H), 2.35–2.32 (m, 2H), 1.18–1.17 (t, J = 7.2 Hz, 3H); LCMS (ESI) *m/z* 499 $(M+H)^+$. HPLC purity: 99.0%; retention time: 3.77 min.

***N*-(4-((4-Ethylpiperazin-1-yl)methyl)-3-(trifluoromethyl)phenyl)-2-(4-(pyridin-3-yl)-phenoxy)acetamide** (**27**): Synthesized as described in the procedure for **9** using **14** and **21** in 5 % yield as an off-white solid. ^{1}H NMR (DMSO-d_6): δ 10.41 (s, 1H), 8.85 (d, J = 1.8 Hz, 1H), 8.52 (m, 1H), 8.09 (d, J = 1.8 Hz, 1H), 8.04–8.01 (m, 1H), 7.88–7.86 (m, 1H), 7.71–7.67 (m, 3H), 7.46–7.43 (m, 1H), 7.13 (d, J = 8.8 Hz, 2H), 4.79 (s, 2H), 3.54 (s, 2H), 2.38–2.28 (m, 10H), 0.98 (t, J = 7.1 Hz, 3H); ^{13}C NMR (DMSO-d_6): δ 166.9, 157.8, 147.8, 147.1, 137.3, 134.9, 133.4, 132.1, 131.2, 130.0, 128.2, 127.9 - 127.2 (q), 126.9, 125.5, 123.7, 122.9, 122.7, 116.6, 116.5, 115.2, 67.0, 57.3, 52.7, 52.2, 51.4, 11.9. LCMS (ESI) *m/z* 499.25 $(M+H)^+$. HPLC purity: 99.9%; retention time: 1.32 min. Melting point: 111.2 ^{o}C.

***N*-(4-((4-Ethylpiperazin-1-yl)methyl)-3-(trifluoromethyl)phenyl)-2-(4-(pyridin-4-yl)-phenoxy)acetamide** (**28**): Synthesized as described in the procedure for **9** using **14** and **22** in 5 % yield as a solid. ^{1}H NMR (DMSO-d_6): δ 10.43 (s, 1H), 8.l59–8.58 (m, 2H), 8.097–8.09 (m, 1H), 7.92–7.90 (m, 1H), 7.81–7.79 (d, J = 8.8 Hz, 2H), 7.70–7.66 (m, 3H), 7.15–7.13 (d, J = 8.8 Hz, 2H), 4.81 (s, 2H), 3.64 (s, 2H), 3.05–2.79 (m, 10H), 1.17 (bs, 3H); ^{13}C NMR (DMSO-d_6): δ 166.7, 158.6, 150.0, 146.2, 137.2, 132.1, 131.2, 129.8, 128.0, 127.2, 125.5, 122.9, 120.5, 116.5, 115.2, 66.9, 57.3, 52.7, 52.2, 51.4, 11.9.LCMS (ESI) MS *m/z* 499 $(M+H)^+$; HPLC purity: 98.3%; retention time: 3.43 min. Melting point: 210.9 ^{o}C.

5-(4-(2-((4-((4-Ethylpiperazin-1-yl)methyl)-3-(trifluoromethyl)phenyl)amino)-2-oxoethoxy)phenyl)-*N*-methylpicolinamide (**29**): Synthesized as described in the procedure for **9** using **14** and **23** in 17 % yield as a solid. ^{1}H NMR (DMSO-d_6): δ 10.40 (s, 1H), 8.78 (s, 1H), 8.74-8.72 (d, J = 4.8 Hz, 1H), 8.21-8.19 (d, J = 8.0 Hz, 1H), 8.04-8.09 (m, 2H), 7.88-7.85 (d, J = 8.8 Hz, 1H), 7.80-7.78 (d, J = 8.4 Hz, 2H), 7.68-7.66 (d, J =8.4 Hz, 1H), 7.15-7.13 (d, J = 8.4 Hz, 2H), 4.81 (s, 2H), 3.54 (s, 2H), 2.82-2.81 (d, J = 4.8 Hz, 3H), 2.27-2.37 (m, 10H), 0.97-0.93 (t, J = 7.0 Hz, 3H); ^{13}C NMR (DMSO-d_6): δ 166.8, 164.1, 158.2, 148.2, 145.8, 137.3, 137.1, 134.6, 132.1, 131.2, 129.0, 128.3, 127.8 - 126.9 (q), 125.5, 122.9, 122.7, 121.7, 116.6, 116.5, 115.3, 66.9, 57.3, 52.7, 52.2, 51.4, 25.9, 11.9. LCMS (ESI) *m/z* 556.21 $(M+H)^+$. HPLC purity: 99.9%; retention time: 4.87 min. Melting point: 192 ^{o}C.

2-(4-(6-Acetamidopyridin-3-yl)phenoxy)-*N*-(4-((4-ethylpiperazin-1-yl)methyl)-3-(trifluoromethyl)phenyl)acetamide (**30**): A mixture of (6-acetamidopyridin-3-yl)boronic acid (40.24 mg, 0.23 mmol), **24** (100 mg, 0.19 mmol), PCy_3 (1.3 mg, 0.0047 mmol), $Pd_2(dba)_3$ (2.0 mg, 0.0019 mmol) and 1.27 M K_3PO_4 (0.26 mL, 0.33 mmol) in 1,4-dioxane (6 mL) was purged with nitrogen gas for 15 minutes. After heating at 100 ^{o}C for 16 h, the reaction mixture was cooled to room temperature, filtered through celite and washed with MeOH (100 mL). The filtrate was concentrated and the residue partitioned between water (50 mL) and EtOAc (50 mL). The aqueous layer was extracted with EtOAc (50 mL). The combined organic extracts were washed with brine (100 mL), dried (Na_2SO_4), concentrated and the residue purified by preparative HPLC to afford **30** (36.2 mg, 33% yield) as a solid. ^{1}HNMR (DMSO-d_6): δ 10.52 (s, 1H), 10.39 (s, 1H), 8.58-8.58 (d, J = 2.0 Hz, 1H), 8.13-8.10 (m, 1H), 8.09-8.08 (d, J = 1.8 Hz, 1H), 8.03-8.00 (dd, J = 8.6, 2.4 Hz, 1H), 7.88-7.86 (d, J = 8.3 Hz, 1H), 7.69-7.65 (m, 3H), 7.11-7.09 (d, J = 8.8 Hz, 2H), 4.77 (s, 2H), 3.54 (s, 2H), 2.37-2.27 (m, 10H), 2.10 (s, 3H), 0.99-0.95

(t, J = 7.1 Hz, 3H); ^{13}C NMR (DMSO-d_6): δ 169.1, 166.9, 157.4, 150.8, 145.1, 137.3, 135.5, 132.1, 131.2, 130.4, 129.8, 128.2, 127.8 – 126.9 (q), 127.5, 125.5, 122.9, 122.8, 116.6, 116.5, 115.2, 115.1, 113.0, 67.0, 5.3, 52.7, 52.2, 51.4, 23.8, 11.9. LCMS (ESI) *m/z*: 556 $(M+H)^+$. HPLC purity: 98.1%; retention time: 4.19 min. Melting point: 204 ^oC.

***N*-(4-(Piperazin-1-ylmethyl)-3-(trifluoromethyl)phenyl)-2-(4-(pyridin-3-yl)phenoxy)-acetamide** (**31**): To a solution of **25** (250 mg, 0.437 mmol), pyridine-3-boronic acid (64 mg, 0.52 mmol) and K_3PO_4 (185 mg, 0.87 mmol) in dioxane:water (8:2 mL) was added $Pd_2(dba)_3$ (12 mg, 0.01 mmol) and PCy_3 (4 mg, 0.01 mmol). After degassing with Argon for 5 minutes, the reaction mixture was heated at 100 °C for 15 h. After cooling to room temperature, water (15 mL) was added to the reaction mixture and extracted with EtOAc (3 x 20 mL). The organic layer was dried over anhydrous Na_2SO_4 and concentrated under reduced pressure. The crude compound was purified by column chromatography over silica gel (100-200 mesh) using a solvent gradient of 15-20% EtOAc in pet-ether as eluent to afford 240 mg of *tert*-butyl 4-(4-(2-(4-(pyridin-3-yl)phenoxy)acetamido)-2-(trifluoromethyl)benzyl)-piperazine-1-carboxylate which was dissolved in CH_2Cl_2 and treated with TFA (2 mL). After 2 h at room temperature, the reaction mixture was concentrated under reduced pressure and the residue partitioned between water and EtOAc. The aqueous layer was basified with sat. $NaHCO_3$ solution and extracted with EtOAc. The combined organic layer was dried over anhydrous Na_2SO_4 and concentrated under reduced pressure to afford 75 mg (38 % over two steps) of **31** as an off-white solid. ^{1}H NMR (DMSO-d_6): δ 10.41 (s, 1H), 8.86 (s, 1H), 8.52-8.51 (d, J = 1.2 Hz , 1H), 8.09-8.02 (m, 2H), 7.89-7.87 (d, J = 8.4 Hz, 1H), 7.71-7.69 (m, 3H), 7.46-7.43 (m, 1H), 7.14-7.12 (m, 2H) 4.79 (s, 2H), 4.30-4.20 (brs, 1H), 3.53 (s, 2H), 2.81-2.77 (m, 4H), 2.40-2.30 (m, 4H); ^{13}C NMR (DMSO-d_6): δ 166.9, 157.8, 147.8, 147.1, 137.3, 134.9, 133.4, 131.9, 131.3, 130.0, 128.2, 127.9, 127.8--

126.9 (q), 125.5, 123.6, 122.9, 122.7, 116.6, 116.5, 116.4, 115.2, 79.0, 67.0, 57.8, 53.1, 44.9. LCMS (ESI) *m/z*: 471.29 $(M+H)^+$. HPLC purity: 99.0%; retention time: 5.91 min. Melting point: 73.5 ^oC.

2-(4-Bromophenoxy)-*N*-(4-((4-ethylpiperidin-1-yl)methyl)-3-(trifluoromethyl)phenyl)-acetamide (**34**): To a stirred solution of **32** (0.7 g, 6.34 mmol) and **33** (1.0 g, 5.29 mmol) in 80 mL of MeOH:THF (1:1) was added AcOH (5 mL) at room temperature. After 2 h, $NaBH_3CN$ (0.98 g, 15.8 mmol) was added and stirring was continued at room temperature for 16 h. The reaction mixture was poured into water (50 mL) and extracted with EtOAc (2 x 30 mL). The combined organic layers were washed with water, brine, dried (Na_2SO_4) and concentrated under reduced pressure. The crude product was purified by column chromatography (silica gel, eluent EtOAc:hexane 7:3) to afford 400 mg of 4-((4-ethylpiperidin-1-yl)methyl)-3-(trifluoromethyl)aniline which was added to a solution of 2-(4-bromophenoxy)acetic acid **19** (0.4 g, 1.73 mmol) in THF (20 mL) containing HATU (1.3 g, 3.46 mmol) and DIPEA (1.15 mL, 6.8 mmol) at room temperature. After 2 h, the reaction mixture was poured into water (1x50 mL) and extracted with EtOAc (1x50 mL). The combined organic layers were washed brine, dried (Na_2SO_4), filtered and concentrated under reduced pressure. The crude product was purified by column chromatography (silica gel, eluent EtOAc:hexane 3:7) to afford **34** (480 mg, 18% over two steps). ^1H NMR ($CDCl_3$): δ 8.23 (s, 1H), 7.75-7.79 (m, 3H), 7.45-7.47 (d, J = 8.0 Hz, 2H), 6.88-6.90 (d, J = 8.0 Hz, 2H), 4.59 (s, 2H), 3.58 (s, 2H), 2.80-2.83 (m, 2H), 1.97-2.02 (m, 2H), 1.64-1.67 (m, 2H), 1.15-1.48 (m, 5H), 0.88 (t, J = 7.5 Hz, 3H); LCMS (ESI) *m/z* 499 $(M+H)^+$.

***N*-(4-((4-Ethylpiperidin-1-yl)methyl)-3-(trifluoromethyl)phenyl)-2-(4-(pyridin-3-yl)-phenoxy)acetamide** (**35**): To a solution of **34** (480 mg, 0.96 mmol) in dioxane:water (20 mL, 9:1) was added pyridine-3-boronic acid (170 mg, 1.44 mmol), K_3PO_4 (400 mg, 1.92 mmol),

$Pd_2(dba)_3$ (26 mg, 0.028 mmol) and PCy_3 (8.4 mg, 0.028 mmol) and the reaction mixture was heated at 100 ^oC under Argon. After 16 h, the reaction mixture was poured into water (50 mL) and extracted with EtOAc (2x30 mL). The combined organic layer was washed with water, brine, dried (Na_2SO_4), filtered and concentrated under reduced pressure. The crude residue was purified by column chromatography (neutral alumina, eluent EtOAc:hexane 1:3) to afford **35** (190 mg, 40 %) as an off-white solid. ^1H NMR ($CDCl_3$): δ 8.82 (s, 1H), 8.57 (s, 1H), 8.31 (s, 1H), 7.85-7.82 (m, 4H), 7.58 (d, *J* = 8.0 Hz, 2H), 7.35 (t, *J* = 8.0 Hz, 1H), 7.12 (d, *J* = 8.0 Hz, 2H), 4.68 (s, 2H), 3.58 (s, 2H), 2.82 (d, *J* = 8.0 Hz, 2H), 2.00 (t, *J* = 8.0 Hz, 2H), 1.66 (d, *J* = 12.0 Hz, 2H), 1.54-1.25 (m, 5H), 0.89 (t, *J* = 8.0 Hz, 3H); ^{13}C NMR (DMSO-d_6): δ 166.8, 157.8, 147.8, 147.1, 137.1, 134.9, 133.4, 132.6, 131.0, 130.0, 128.2, 127.9, 127.7 - 126.8 (q), 125.5, 123.7, 122.9, 122.8, 116.5, 116.4, 115.2, 67.0, 57.6, 53.4, 36.8, 31.6, 28.6, 11.0. LCMS (ESI) *m/z* 498 $(M+H)^+$. HPLC purity: 98.6%; retention time: 6.36 min. Melting point: 157 ^oC.

1-Ethyl-4-(4-nitro-2-(trifluoromethyl)benzylidene)piperidine (**37**): To a solution of **36** (0.25 g, 0.88 mmol) in toluene (2 mL) was added triethyl phosphite (0.17 g, 1.06 mmol). After heating at 100 ^oC for 16 h, the reaction mixture was cooled to room temperature and evaporated. The residue was purified by column chromatography (silica gel, elueting with EtOAc:hexane 1:1) to afford diethyl 4-nitro-2-(trifluoromethyl)benzylphosphonate (0.3 g, 0.88 mmol) which was dissolved in THF (20 mL) and treated sequentially with NaH (60% in mineral oil, 70.4 mg, 1.76 mmol) and 1-ethylpiperidin-4-one (0.13 mL, 0.97 mmol) at 0 ^oC. After 16 h at room temperature, the reaction mixture was poured into water and extracted with EtOAc (2x50 mL). The combined organics were washed with water, brine, dried (Na_2SO_4), filtered and concentrated to afford **37** (150 mg, 55%). ^1H NMR (DMSO-d_6): δ 8.55 (s, 1H), 8.37-8.39 (d, *J* = 8.0 Hz, 1H), 7.41-7.43 (d,

J = 8.0 Hz, 1H), 6.60 (s, 1H), 4.07-4.15 (m, 4H), 2.68-2.94 (m, 6H), 1.32-1.35 (t, *J* = 7.0 Hz, 3H); LCMS (ESI) *m/z* 315.2 $(M+H)^+$.

***N*-(4-((1-Ethylpiperidin-4-yl)methyl)-3-(trifluoromethyl)phenyl)-2-(4-(pyridin-3-yl)phenoxy)acetamide** (**38**): **37** (150 mg, 0.48 mmol) was dissolved in 50 mL of EtOH and was hydrogenated at 50 psi with 15 mg of Pt/C at room temperature for 5 h. The reaction mixture was filtered through celite and washed with EtOH. The filtrate was evaporated under reduced pressure and the residue was added to a solution of 2-(4-(pyridin-3-yl)phenoxy)acetic acid (0.080 g, 0.35 mmol) in DMF (20 mL) containing DIPEA (0.19 mL, 1.05 mmol) and HATU (0.2 g, 0.52 mmol). After 16 h at room temperature, the reaction mixture was poured into water (100 mL) and extracted with EtOAc (2x50 mL). The combined organic layer was washed with water, brine, dried (Na_2SO_4) and concentrated. The residue was purified by preparative HPLC to afford **38** (25 mg, 11 % over two steps) as a white solid. ^{1}H NMR (DMSO-d_6): δ 10.37 (s, 1H), 8.86 (s, 1H), 8.52 (d, *J* = 4.0 Hz, 1H), 8.02-8.06 (m, 2H), 7.84 (d, *J* = 8.4 Hz, 1H), 7.71 (d, *J* = 4.2 Hz, 2H), 7.40-7.47 (m, 2H), 7.14 (d, *J* = 8.8 Hz, 2H), 4.79 (s, 2H), 2.82 (d, *J* = 11 Hz, 2H), 2.60-2.67 (m, 2H), 2.23-2.33 (m, 2H), 1.74 (t, *J* = 11.2 Hz, 2H), 1.49-1.52 (m, 3H), 1.18-1.24 (m, 2H), 0.96 (t, *J* = 7.0 Hz, 3H); ^{13}C NMR (DMSO-d_6): δ 166.8, 157.8, 147.7, 147.1, 136.5, 134.9, 134.1, 133.6, 133.4, 132.4, 130.2, 130.0, 127.9, 127.8 - 126.9 (q), 125.6, 123.7, 122.9, 122.8, 116.7, 116.6, 115.2, 67.0, 52.7, 51.6, 38.0, 37.1, 31.6, 12.0. LCMS (ESI) *m/z* 498.08 $(M+H)^+$. HPLC purity: 96.4%; retention time: 6.21 min. Melting point: 148 ^{o}C.

***N*-(3-Cyclopropyl-4-((4-ethylpiperazin-1-yl)methyl)phenyl)-2-(4-(pyridin-3-yl)phenoxy)-acetamide** (**40**): To a solution of **39** (1.0 g, 3.05 mmol), cyclopropyl boronic acid (0.28 g, 3.35 mmol) and K_2CO_3 (0.84 g, 6.11 mmol) in 1,4-dioxane (9 mL) containing water (1 mL) was added $Pd(dppf)Cl_2.CH_2Cl_2$ (0.12 g, 0.15 mmol) and the reaction mixture was degassed with

argon for 5 min. After 16 h at 100 °C, the reaction mixture was diluted with water and extracted with EtOAc (3x20 mL). The organic layer was separated, dried (Na_2SO_4), filtered and evaporated. The residue was purified by column chromatography over silica gel (60-120 mesh) eluting with EtOAc:hexane (1:5) to afford 0.4 g of 1-(2-cyclopropyl-4-nitrobenzyl)-4-ethylpiperazine [LCMS (ESI) *m/z* 290.12] which was dissolved in MeOH (20 mL) and treated with $NiCl_2.6H_2O$ (0.65 g, 2.7 mmol) and $NaBH_4$ (0.2 g, 5.3 mmol) at 0 °C. After 4 h, the reaction mixture was diluted with water and extracted with EtOAc (3x15 mL). The organic layer was separated, dried (Na_2SO_4), filtered and evaporated. The residue was purified by column chromatography (silica gel 60-120 mesh) eluting with EtOAc:hexane (1:5) to afford 3-cyclopropyl-4-((4-ethylpiperazin-1-yl)methyl)aniline (0.19 g, 0.84 mmol) which was added to a solution of 2-(4-(pyridin-3-yl)phenoxy)acetic acid (0.2 g, 0.77 mmol) in dry THF (2 mL) containing HATU (0.44 g, 1.15 mmol) and DIPEA (0.27 mL, 1.54 mmol). After 6 h at room temperature, the reaction mixture was diluted with water and extracted with EtOAc (3x20 mL). The organic layer was separated, dried (Na_2SO_4), filtered and evaporated. The crude compound was triturated with CH_2Cl_2 to afford **40** (0.034 g, 2 % over three steps) as an off-white solid. ^{1}H NMR: (DMSO-d_6): δ 9.97 (br s, 1H), 8.85 (br s, 1H), 8.51-8.52 (d, J = 3.6 Hz, 1H), 8.01-8.03 (d, J = 8.0 Hz, 1H), 7.68-7.70 (d, J = 8.0 Hz, 2H), 7.43-7.46 (m, 2H), 7.10-7.21 (m, 4H), 4.73 (s, 2H), 3.52 (s, 2H), 2.15-2.50 (m, 11H), 0.98-0.90 (m, 5H), 0.54-0.55 (d, J = 4.0 Hz, 2H); ^{13}C NMR (DMSO-d_6): δ 166.1, 157.9, 147.7, 147.2, 142.3, 137.2, 135.0, 133.4, 132.5, 129.9, 129.7, 123.7, 116.3, 116.0, 115.5, 67.0, 59.2, 52.7, 52.4, 51.5, 12.1, 11.9, 7.4. LCMS (ESI) *m/z* 471.20 $(M+H)^+$. HPLC purity: 95.4%; retention time: 5.55 min. Melting point: 132.5 ^{o}C.

***N*-(4-((4-Ethylpiperazin-1-yl)methyl)-3-(trifluoromethyl)phenyl)-2-(4-(pyridin-3-yl)phenoxy)propanamide** (**42**): A mixture of ethyl 2-(4-iodophenoxy)propanoate **41** (0.85 g,

2.67 mmol) and pyridine-3-boronic acid (0.33 g, 2.67 mmol) in 1,4-dioxane (6 mL) containing 2M Na_2CO_3 (5.35 mL, 10.7 mmol) was degassed with nitrogen for 10 minutes. $Pd(PPh_3)_4$ (0.3 g, 0.26 mmol) was subsequently added and the reaction mixture was again degassed with N_2 for another 10 minutes before it was heated at 100 ^oC for 16 h. The reaction mixture was cooled to room temperature, filtered through celite and evaporated under reduced pressure. The residue was partitioned between water and EtOAc. The organic layer was washed with brine, filtered, dried (anh. Na_2SO_4) and evaporated. The crude product [0.34 g, LCMS (ESI) *m/z* 244 $(M+H)^+$] was added to a solution of **14** (0.20 g, 0.70 mmol) and HATU (0.535 g, 1.41 mmol) in DMF (4 mL) containing Et_3N (0.4 mL, 2.81 mmol). After stirring at room temperature for 1.5 h, the reaction mixture was poured into water and extracted with EtOAc (3x20 mL). The combined organic layers were washed with brine, dried (Na_2SO_4) and evaporated under reduced pressure. The residue was purified by preparative HPLC eluting with 10%-30%-95% MeCN containing 0.1% formic acid. The fractions containing the compound were evaporated and the residue partitioned between CH_2Cl_2 and sat. $NaHCO_3$ solution. The organic layer was washed with brine, dried over sodium sulfate and evaporated under reduced pressure to yield **42** (23.3 mg, 2 % over two steps) as a white solid. ^{1}HNMR (DMSO-d_6): δ 10.47 (s, 1H), 8.84-8.83 (d, J = 1.6 Hz, 1H), 8.51-8.50 (d, J = 4.8, 1,6 Hz, 1H), 8.08-8.07 (d, J = 1.6 Hz, 1H), 8.01-7.99 (m, 1H), 7.88-7.86 (d, J = 8.4, 1.6 Hz, 1H), 7.69-7.66 (m, 3H), 7.45-7.41 (m, 1H), 7.09-7.07 (d, J = 7.2 Hz, 2H), 4.99-4.93 (q, J = 13.2, 6.4 Hz, 1H), 3.53 (s, 2H), 2.36-2.26 (m, 10H), 1.59-1.58 (d, J = 6.4 Hz, 3H), 0.99-0.95 (t, J = 7.2 Hz, 3H); ^{13}C NMR (DMSO-d_6): δ 170.3, 157.2, 147.7, 147.1, 137.4, 134.9, 133.4, 132.1, 131.2, 130.0, 128.2, 128.0, 127.8 - 126.9 (q), 125.5, 123.6, 122.8, 122.7, 120.0, 116.5, 116.4, 115.6, 73.7, 57.3, 52.6, 52.2, 51.4, 18.4, 11.9. LCMS (ESI) *m/z* 513 $(M+H)^+$. HPLC purity: 99.2%; retention time: 3.77 min. Melting point: 190 ^oC.

***Tert*-butyl (4-bromophenyl)(2-((4-((4-ethylpiperazin-1-yl)methyl)-3-(trifluoromethyl)-phenyl)amino)-2-oxoethyl)carbamate** (**46**): To a solution of **44** (0.2 g, 0.60 mmol), HATU (0.25 g, 0.66 mmol) and Et_3N (0.23 mL, 1.68 mmol) in THF (5 mL) was added **14** (0.17 g, 0.6 mmol). After stirring at room temperature for 14 h, the reaction mixture was diluted with water and extracted with EtOAc (3x20 mL). The organic layer was washed with brine, dried (Na_2SO_4), filtered and concentrated under reduced pressure. The residue was subjected to silica gel column chromatography eluting with 1% MeOH in $CHCl_3$ containing 1 mL Et_3N to afford **46** (0.2 g, 55% yield) as a semi-solid. ^{1}H NMR ($CDCl_3$): δ 10.40 (s, 1H), 8.05 (s, 1H), 7.77-7.66 (m, 2H), 7.54-7.51 (d, *J* = 8.4 Hz, 2H), 7.32-7.29 (d, *J* = 8.4 Hz, 2H), 4.34 (s, 2H), 3.53 (s, 2H), 3.42 (br s, 2H), 2.58-2.32 (m, 8H), 1.44 (s, 9H), 0.99-0.96 (t, *J* = 7.2 Hz, 3H); LCMS (ESI) *m/z* 599.3 $(M+H)^+$.

In a similar manner, ***tert*-butyl 4-(4-(2-((4-bromophenyl)(tert-butoxycarbonyl)amino)-acetamido)-2-(trifluoromethyl)-benzyl)piperazine-1-carboxylate** (**47**) was synthesized from **44** and **18** in 66% yield as a pale brown oil. ^{1}H NMR ($CDCl_3$): δ 8.43 (s, 1H), 7.68-7.76 (m, 3H), 7.47-7.45 (d, *J* = 8.8 Hz, 2H), 7.20-7.18 (d, *J* = 8.8 Hz, 2H), 4.31 (s, 2H), 3.60 (s, 2H), 3.42 (br s, 4H), 2.40 (br s, 4H), 1.58 (s, 9H), 1.48 (s, 9H); LCMS (ESI) *m/z* 671.1 and 673.2 $(M+H)^+$.

***N*-(4-((4-ethylpiperazin-1-yl)methyl)-3-(trifluoromethyl)phenyl)-2-((4-(pyridin-3-yl)-phenyl)amino)acetamide** (**48**): A solution of **46** (600 mg, 1.0 mmol), pyridine-3-boronic acid (123 mg, 1.0 mmol) and K_2CO_3 (272 mg, 2.0 mmol) in dioxane-water (4:1 mL) under argon atmosphere was added Pd(dppf)CH_2Cl_2 (41 mg, 0.05 mmol) and degassed with argon for another 10 min. After 100 °C for 5 h, the reaction mixture was cooled to room temperature and diluted with EtOAc. The combined organic layer was washed with water, brine, dried over anhydrous Na_2SO_4 and concentrated under reduced pressure. The residue was filtered through c neutral

alumina using 1% MeOH:$CHCl_3$ as eluent and concentrated. The crude product was dissolved in CH_2Cl_2 and treated with TFA (3 mL) at room temperature for 3 h. The reaction mixture was concentrated under reduced pressure, diluted with water, and washed with EtOAc. The aqueous layer was basified with saturated $NaHCO_3$ solution. Solid separated was filtered, washed with water and dried to afford **48** (25 mg, 5% yield over two steps). ^{1}H NMR (DMSO-d_6): δ 10.32 (s, 1H), 8.79-8.75 (m, 1H), 8.43-8.41 (m, 1H), 8.07-8.07 (m, 1H), 7.94-7.91 (m, 1H), 7.83-7.81 (m, 1H), 7.67-7.65 (m, 1H), 7.51-7.49 (d, *J* = 8.8 Hz, 2H), 7.39-7.36 (m, 1H), 6.72-6.70 (d, *J* = 8.8 Hz, 2H), 6.35-6.32 (t, *J* = 6.4 Hz, 1H), 3.95-3.93 (d, *J* = 6.4 Hz, 2H), 3.52-3.50 (m, 3H), 2.36-2.26 (m, 9H), 0.98-0.95 (t, *J* = 7.2 Hz, 3H); LCMS (ESI) *m/z* 498 $(M+H)^+$. HPLC purity: 98.7%; retention time: 3.24 min.

In a similar manner, the following compounds were synthesized:

2-(4-(6-Acetamidopyridin-3-yl)phenylamino)-*N*-(4-((4-ethylpiperazin-1-yl)methyl)-3-(trifluoromethyl)-phenyl)acetamide (**49**): Synthesized in 51 % yield (over two steps) as an off-white solid. (6-Acetamidopyridin-3-yl)boronic acid was used for Suzuki coupling with **46**. ^{1}H NMR (CD_3OD): δ 8.45 (d, *J* = 1.7 Hz, 1H), 8.07 (d, *J* = 8.8 Hz, 1H), 8.00 (d, *J* = 1.8 Hz, 1H), 7.92 (dd, *J* = 12, 2.6 Hz, 1H), 7.69-7.78 (m, 2H), 7.45 (d, *J* = 8.8 Hz, 2H), 7.76 (d, *J* = 8.8 Hz, 2H), 3.97 (s, 2H), 3.62 (s, 2H), 2.42-2.70 (m, 10H), 2.17 (s, 3H), 1.10 (t, *J* = 7.3 Hz, 3H); ^{13}C NMR (DMSO-d_6): δ 169.6, 168.9, 150.0, 147.9, 144.3, 137.7, 134.6, 131.6, 131.3, 131.2, 127.8 - 126.9 (q), 126.8, 125.5, 124.7, 122.8, 122.4, 116.1, 116.0, 113.0, 112.7, 69.6, 57.3, 52.7, 52.2, 51.4, 47.0, 23.7, 11.9. LCMS (ESI) *m/z* 553.3 $(M-H)^+$. HPLC purity: 99.8%; retention time: 3.80 min. Melting point: 234.5 ^{o}C.

2-((4-(6-Acetamidopyridin-3-yl)phenyl)amino)-*N*-(4-(piperazin-1-ylmethyl)-3-(trifluoromethyl)phenyl)acetamide (50): Synthesized in 12% yield over two steps as a white solid. (6-Acetamidopyridin-3-yl)boronic acid was used for Suzuki coupling with **47**. ^{1}H NMR (DMSO-d_6): δ 10.44 (s, 1H), 10.32 (s, 1H), 8.51-8.50 (d, J = 2 Hz, 1H), 8.07-8.05 (m, 2H), 7.94-7.92 (dd, J = 8.8, 2.8 Hz, 1H), 7.83-7.81 (dd, J = 8.4, 1.6 Hz, 1H), 7.68-7.66 (d, J = 8.4 Hz, 1H), 7.47-7.45 (d, J = 8.4 Hz, 2H), 6.70-6.68 (d, J = 8.4 Hz, 2H), 6.27-6.24 (t, J = 6.0 Hz, 1H), 3.93-3.92 (d, J = 5.6 Hz, 2H), 3.48 (s, 2H), 2.67-2.55 (m, 4H), 2.30-2.27 (m, 4H), 2.08 (s, 3H); ^{13}C NMR (DMSO-d_6): δ 169.6, 168.9, 150.0, 147.9, 144.3, 137.7, 134.6, 131.6, 131.3, 131.2, 127.5 (q), 126.8, 124.7, 122.4, 116.0, 113.0, 112.7, 58.0, 53.9, 47.0, 45.4, 23.7. LCMS (ESI) *m/z* 527.2 $[M+H]^+$. HPLC purity: 99.4%; retention time: 4.75 min. Melting point: 180.5 ^{o}C.

***N*-(5-(4-((2-Oxo-2-((4-(piperazin-1-ylmethyl)-3-(trifluoromethyl)phenyl)amino)-ethyl)amino)-phenyl)pyridin-2-yl)isobutyramide** (**51**): Synthesized in 10 % yield (over two steps) as a white solid. **55** was used for Suzuki coupling with **47**. ^{1}H NMR (DMSO-d_6): δ 10.37 (s, 1H), 10.31 (s, 1H), 8.50 (s, 1H), 8.06-8.10 (m, 2H), 7.92-7.95 (m, 1H), 7.82 (d, J = 8.0 Hz, 1H), 7.67 (d, J = 8.0 Hz, 1H), 7.46 (d, J = 8.8 Hz, 2H), 6.69 (d, J = 8.8 Hz, 2H), 6.26 (t, J = 6.0 Hz, 1H), 3.92-3.94 (m, 2H), 3.49 (br s, 2H), 2.67-2.76 (m, 5H), 2.27-2.33 (m, 4H), 1.09 (d, J = 6.8 Hz, 6H); LCMS (ESI) *m/z* 555.19 $(M+H)^+$. HPLC purity: 97.7%; retention time: 4.55 min. Melting point: 171.5 ^{o}C.

***N*-(5-(4-((2-Oxo-2-((4-(piperazin-1-ylmethyl)-3-(trifluoromethyl)phenyl)amino)ethyl)-amino)phenyl)pyridin-2-yl)cyclopropanecarboxamide (52)**: Synthesized in 11 % yield over two steps as an off-white solid. **56** was used for Suzuki coupling with **47**. ^{1}H NMR (DMSO-d_6): δ 10.77 (s, 1H), 10.32 (s, 1H), 8.50 (s, 1H), 8.07–8.05 (m, 2H), 7.94–7.91 (m, 1H), 7.83–7.81 (d, J = 8.5 Hz, 1H), 7.68–7.66 (d, J = 8.6 Hz, 1H), 7.47–7.45 (d, J = 8.6 Hz, 2H), 6.70–6.68 (d, J =

8.6 Hz, 2H), 6.29–6.27 (t, *J* = 6.8 Hz, 1H), 3.94–3.92 (d, *J* = 6.1 Hz, 2H), 3.49 (s, 2H), 2.69–2.67 (m, 4H), 2.28 (br s, 4H), 2.03 (m, 1H), 0.79-0.80 (m, 4H); ^{13}C NMR (DMSO-d_6): δ 172.2, 169.6, 150.0, 147.9, 144.3, 137.7, 134.6, 131.6, 131.3, 131.2, 127.7 – 126.9 (q), 126.8, 125.5, 124.7, 122.8, 122.4, 116.1, 116.0, 113.1, 112.7, 58.0, 54.0, 47.0, 45.4, 14.0, 7.4. LCMS (ESI) *m/z* 551.2 $(M-H)^+$. HPLC purity: 98.1%; retention time: 6.55 min. Melting point: 227.1 ^oC.

***N*-(5-(4-((2-((4-((4-Ethylpiperazin-1-yl)methyl)-3-(trifluoromethyl)phenyl)amino)-2-oxoethyl)amino)phenyl)pyridin-2-yl)cyclopropanecarboxamide** (**53**): Synthesized in 47 % yield as an off-white solid using **56** as coupling partner with **46**. ^{1}H NMR (DMSO-d_6): δ 10.76 (s, 1H), 10.31 (s, 1H), 8.51 (d, *J* = 2.0 Hz, 1H), 8.06 (s, 1H), 8.04-8.02 (d, *J* = 8.8 Hz, 1H), 7.93-7.90 (dd, *J* = 8.8, 2.0 Hz, 1H), 7.83-7.81 (d, *J* = 8.0 Hz, 1H), 7.67-7.65 (d, *J* = 8.0 Hz, 1H), 7.47-7.45 (d, *J* = 8.4 Hz, 2H), 6.70-6.68 (d, *J* = 8.4 Hz, 2H), 6.27-6.24 (t, *J* = 5.6 Hz, 1H), 3.94-3.92 (d, *J* = 5.6 Hz, 2H), 3.50 (s, 2H), 2.34 (m, 8H), 2.32-2.26 (q, *J* = 14.4, 7.2 Hz, 2H), 2.01-1.97 (m, 1H), 0.98-0.96 (t, *J* = 7.2 Hz, 3H), 0.78 (m, 4H); ^{13}C NMR (DMSO-d_6): δ 172.3, 169.7, 150.1, 148.0, 144.4, 137.8, 134.6, 131.6, 131.3, 127.5-126.8 (q) , 125.6, 124.8, 122.8, 122.5, 116.1, 113.1, 112.8, 57.3, 52.7, 52.3, 51.5, 47.1, 14.1, 11.8, 7.5; LCMS (ESI) *m/z* 581.33 $(M+H)^+$. HPLC purity: 98.3%; retention time: 4.20 min. Melting point: 238.8 ^oC.

***N*-(5-(3-Fluoro-4-((2-((4-((4-methylpiperazin-1-yl)methyl)-3-(trifluoromethyl)phenyl)-amino)-2-oxoethyl)amino)phenyl)pyridin-2-yl)cyclopropanecarboxamide** (**54**): A stirred solution of **45** (6.0 g, 17.29 mmol) in THF (100 mL) was treated with **43** (8.2 g, 17.29 mmol), HATU (9.8 g, 25.93 mmol) and Et_3N (4.8 mL, 34.58 mmol) at room temperature and stirred for 16 h. Solvent was evaporated and the reaction mixture was diluted with EtOAc (300 mL). Organic layer was washed with water (100 mL) and brine (100 mL), dried (anh. Na_2SO_4), filtered and evaporated. The crude residue was dissolved in dioxane-water (80 mL, 3:1). After

the addition of **56** (7.3 g, 25.53 mmol), K_2CO_3 (6.3 g, 46.43 mmol) and Pd(dppfCl_2).CH_2Cl_2 (0.950 mg, 1.16 mmol), the reaction mixture was degassed with Argon for 20 min. and heated at 100 °C for 3 h. After cooling to room temperature, the reaction mixture was evaporated under reduced pressure and the residue diluted with water (40 mL) and extracted with EtOAc (3x100 mL). The organic layer was washed with brine (1x100 mL), dried over anhydrous Na_2SO_4, filtered and evaporated. The crude product was purified by column chromatography over neutral silica gel using EtOAc as eluent to afford 9 g of *tert*-butyl (4-(6-(cyclopropanecarboxamido)pyridin-3-yl)-2-fluorophenyl)(2-((4-((4-methylpiperazin-1-yl)methyl)-3-(trifluoromethyl)phenyl)amino)-2-oxoethyl)-carbamate (ESI MS: *m/z* 685 $[M+H]^+$) which was dissolved in CH_2Cl_2 (80 mL) and was treated with TFA (40 mL) at room temperature. After stirring at room temperature for 2 h, the reaction mixture was concentrated and diluted with water (50 mL). The aqueous layer was washed with diethyl ether (100 mL), basified with $NaHCO_3$ solution and extracted with EtOAc (2x200 mL). The combined organic layer was dried (anh. Na_2SO_4), filtered and concentrated. Purification of the residue by preparative HPLC gave 2.5 g (25% yield over three steps) of **54** as an off-white solid. ^{1}H NMR (DMSO-d_6): δ 10.80 (s, 1H), 10.34 (s, 1H), 8.57-8.56 (d, J = 2.0 Hz, 1H), 8.08-8.06 (d, J = 8.4 Hz, 1H), 8.059 (s, 1H), 7.99-7.96 (dd, J = 8.4, 2.0 Hz, 1H), 7.82-7.80 (d, J = 8.0 Hz, 1H), 7.66-7.64 (d, J = 8.0 Hz, 1H), 7.51-7.47 (dd, J = 12.8, 2.0 Hz, 1H), 7.37-7.35 (d, J = 8.0 Hz, 1H), 6.73-6.68 (t, J = 8.4 Hz, 1H), 6.02-6.00 (t, J = 6.0 Hz, 1H), 4.02-4.00 (d, J = 6.0 Hz, 2H), 3.53 (s, 2H), 2.36-2.32 (m, 8H), 2.14 (s, 3H), 2.04-1.98 (m, 1H), 0.90-0.85 (m, 4H); ^{13}C NMR (DMSO-d_6): δ 172.4, 169.3, 158.2, 157.9 , 152.4, 150.5, 150.0, 144.7, 138.0, 136.0, 135.9, 134.9, 131.4, 131.1, 130.0, 127.7-127.4 (q), 125.5, 125.1, 122.8, 122.5, 122.4, 116.2, 113.1, 112.4, 112.3, 112.2, 56.9, 53.6, 50.9, 46.6,

43.8, 40.1, 14.1, 7.6; LCMS (ESI) *m/z* 585 $[M+H]^+$. HPLC purity: 99.9%; retention time: 4.59 min. Melting point: 196.5 ^oC.

Protein expression, purification, activation of MNK1 and MNK2: The amino acid sequences of the kinase domains of MNK1 (amino acids 37-341) and MNK2 (amino acids 72-385) were reverse translated and codon optimized for expression in *E.coli*. The genes were synthesized and cloned into the expression vector pGEX6P containing a *N*-terminal GST tag by GenScript USA Inc. The plasmids were transformed into BL21 (DE3) cells. MNK1 and MNK2 were induced with 1.0 mM IPTG and grown at 25°C for 6 h. The proteins were purified using affinity chromatography on a Bio-Scale Mini Profinity GST cartridge. The GST tag was cleaved using Thrombin Cleavage Capture Kit.

The amino acid sequences of MEK1 (amino acids 2-293) and ERK2 (amino acids 2-360) were reverse translated and codon optimized for expression in *E. coli*. In order to generate a constitutively active kinase, Serine 218 and Serine 222 of the MEK1 DNA sequence were replaced with glutamic acid residues. The genes were synthesized and cloned into the expression vector pQE80L containing a *N*-terminal His6 tag by GenScript USA Inc. The plasmids were transformed into BL21 (DE3) cells. ERK2 and mutant MEK1 are induced with 1.0mM IPTG and grown at 25°C for 5 h. The proteins were purified using affinity chromatography on a Bio-Scale Mini Profinity IMAC cartridge.

Recombinant ERK2 was activated by incubating 11.3 μM of the kinase with 1 μM MEK1 and 100 μM ATP. The activation of the MNK1 was performed by incubating 5.0 μM of MNK1 with 0.3 μM of activated ERK2 and 500 μM ATP at 30°C for 6 h. The activation of MNK2 was

performed by incubating 50μM of MNK2 with 3.0 μM of activated ERK2 and 500 μM ATP at 30°C for 2 h.

***In vitro* MNK1, MNK2, BCR-ABL1 and ABL(T315I) kinase assays:** Caliper EZ Reader II mobility shift assay from Perkin Elmer was utilized for the activity-based assays. Reactions were started by incubation of 6 μL enzyme solution and 10 μL compound in assay buffer (100mM HEPES (pH 7.5), 10 mM $MgCl_2$, 0.004% TWEEN® 20 buffer, 1 mM DTT and 0.003% Brij® L23) for 10 minutes, followed by 10 μL substrate mix containing ATP and 1.5 μM peptide substrate in assay buffer. After incubation for 60 min. at room temperature, the kinase reaction was stopped by the addition of 10 mM EDTA in 45 μL termination buffer. The stopped reaction was analyzed on a LabChip EZ Reader II (Perkin Elmer).

For MNK1 kinase assay, concentrations of MNK1 and ATP were 40 nM and 1.2 mM. For MNK2 kinase assay, concentrations of MNK2 and ATP were 20 nM and 250 μM. JH3 peptide (5FAM-TATKSGSTTKNRFVV-NH2, supplied by GenScript) was used for MNK1 and MNK2 assay.

For BCR-ABL1 kinase assay, concentrations of BCR-ABL1 (Carna biosciences) and ATP were 1 nM and 14 μM. For the ABL^{T315I} kinase assay, concentrations of ABL^{T315I} (Carna biosciences) and ATP were 1.5 nM and 12 μM. FL-peptide 2 (5FAM-EAIYAAPFAKKK-NH2, supplied by GenScript) was used for BCR-ABL1 and ABL^{T315I} assay. IC_{50}s were determined using GraphPad Prism.

***In vitro* Flt3, KIT, PDGFRα, PDGFRβ, FGFR2, RET and VEGFR2 kinase assays:** These assays were carried out at Eurofins Pharma Discovery Services UK Limited.

MNK Cell-Based Assay

In vitro Alphascreen assay: HeLa cells were obtained from ATCC and cultured in DMEM (Invitrogen) supplemented with 10% (*v/v*) Fetal Bovine Serum (FBS)-US grade (Invitrogen), 100 UmL-1 penicillin (Invitrogen), and 100 gmL-1 streptomycin (Invitrogen). Cells were cultured in a humidified 5% CO2 incubator at 37 °C.

Alphascreen® SureFire® eIF4E p-Ser209 assay– The Alphascreen® SureFire® assay (Perkin Elmer, cat#TGREIF4S500) was performed in 384 well white Proxiplates according to the manufacturer instructions. Cells were seeded at 30,000 cells per well in a 96-well plate and incubated for 24 h before treatment with compounds. After 24 h, the culture media was removed and the cells were treated with compounds that were serial diluted in DMEM media without FBS for 2 hours in a humidified 5% CO_2 incubator at 37 °C prior to cell lysis. At the end of the 2h incubation, the medium was removed and the cells were lysed with freshly prepared 1X lysis buffer (supplied in the Alphascreen® SureFire® Kit) and agitated on a plate shaker at 350 rpm for 20 min. at room temperature. 4 µL of lysate was incubated with 5 µL of Acceptor Mixture for 2 h at room temperature before 2 µL of Donor Mixture was added under subdued lighting. Plates were further incubated for 2 h at room temperature and read with the PerkinElmer EnVision plate reader using AlphaScreen® settings. Raw data were presented as 'alphascreen signals'. Percentage inhibition was calculated based on the % reduction in 'alphascreen sigals' after treatment as compared to DMSO control. IC_{50} measurements were performed using GraphPad Prism Version 5.00 for Windows (Graphpad software, San Diego California USA).

Determination of growth inhibition of BC CML cells: Cancer cell lines K-562, BV-173, EM-2, KCL-22, JURL-MK1 and TMM were purchased from ATCC and cultured according to supplier's recommendations. K562 cells over-expressing eIF4E[6] were also used for the cytotoxicity assay. For cells treated for 48 h, 5000 cells were seeded in 70 µl of growth medium

in black, flat-bottom 96-well plate. The compounds Imatinib, **53** and **54** were treated with doses ranging from 0.003 μM to 50 μM. 50 μL of the diluted compounds was added to the cells and incubated at 37 ^{o}C in 5% CO_2. After 48 h treatment, cell viability was determined by CellTiter-Glo Luminescent Cell Viability Assay (Promega, Madison, WI). 120 μL of the reagent was added to the cells and luminescence was measured using Tecan Safire Reader. Data was analyzed with Graphpad Prism software and the figures represented indicate the half maximal inhibitory concentration (GI_{50}).

Western blot: K562 cells overexpressing eIF4E are treated with 100 nM, 500 nM and 1000 nM of compound for 24 h. The cells are lysed with Ripa Buffer containing SDS and protease and phosphatase inhibitor cocktail (Santa Cruz Biotechnology, Inc). The lysates were quantitated with Quick Start™ Bradford Protein Assay (Bio-Rad) and denatured by boiling with 2X Laemmli sample buffer supplemented with β-mercaptoethanol (Bio-Rad) for 10 min. Equal amounts of protein were loaded and separated using the NuPAGE Novex 4-12% gradient Bis-Tris Protein Gel (Life Technologies) and subsequently transferred to a PVDF membrane. Membrane was blocked for 1 h at room temperature in 5% w/v BSA in PBST. Incubation with primary antibody (anti-eIF4E abcam#130210, anti-eIF4E phosphor-S209 abcam#4774, PathScan® Bcr/Abl Activity Cocktail #5300) were performed overnight at 4 °C followed by secondary antibody (ECL-anti mouse IgG-HRP, GE Healthcare #NA9310 or ECL-anti rabbit IgG-HRP, GE Healthcare #NA9340) incubation for 1 h at room temperature. ECL-Plus (Amersham #RPN2235) were used for western blot detection using the FluorChem R Imaging system (ProteinSimple) Chemiluminescent channel.

Thermodynamic solubility: Thermodynamic solubility of compounds were determined as reported earlier.[35]

***In Vivo* Antitumor Efficacy Studies**: Severe combined immunodeficient (C.B-Igh-1b/IcrTac-Prkd-scid) female mice 7 to 10 weeks old were purchased from Biolasco, Taiwan. Animals were maintained under specific pathogen-free conditions and had access to sterile food and water ad libitum. All animal studies were conducted at the Biological Research Centre, Singapore, with the prior approval of the local Institutional Animal Care Committee (BRC-IACUC approval no. 110622).

53 and **54** were weighted and dissolved in 0.5%MC/0.1% TW80 solution. The mixtures were vortexed and sonicated in the ultrasonic bath for 30 min. The final concentration of **53** and **54** dosing solution was 5, 10 and 20 mg/mL for oral dosing at 50, 100 and 200 mg/kg, respectively.

K562 cells overexpressing eIF4E were cultured in the RPMI medium supplemented with 10% fetal bovine serum (Life Technologies, Singapore) and antibiotic solution (100 units/mL penicillin and 100 μg/mL streptomycin) at 37 °C under 5% CO_2.

Female SCID mice were subcutaneously injected with 1 x 10^7 K562 overexpressing eIF4E cells. The volume of injection was 100 μL per mouse. After implantation, the tumor was monitored twice per week using a digital caliper. The K562o/e eIF4E tumor volume was estimated following the formula:

Tumor volume (mm^3) = (w^2 x l)/2, where w = width and l = length in mm.

When the tumors attained a tumor volume of between 75 to 245 mm^3, mice were randomly distributed into different groups. After randomization, mice bearing K562-eIF4E tumors received vehicle (0.5% MC/0.1%TW80), **53, 54** or imatinib (imatinib mesylate, LC laboratories) once daily for 14 days (qd x 14) *via* oral gavage. The volume of oral administration was 10 mL/kg. The dosing level for **53** and **54** was 50, 100 and 200 mg/kg. Imatinib was dosed at 200 mg/kg.

The endpoint used to measure the response of the K562 o/e eIF4E tumors after compound treatment was tumor growth inhibition at day 14 and was expressed as %TGI and T/C ratio. The percentage of tumor growth inhibition (%TGI) was calculated as follows:

$$\%TGI = (C_{day\ a} - T_{day\ a})/ (C_{day\ a} - C_{day\ 1}) \times 100$$

Where $C_{day\ a}$ = mean tumor volume of the vehicle control group at the indicated day a; $T_{day\ a}$ = mean tumor volume of the group treated with the test compound at the indicated day a; C_{day1} = mean tumor volume of the vehicle control group at Day 1. The T/C ratio was calculated as follows:

$$T/C\ ratio = T_{day\ a} /C_{day\ a}$$

One-way ANOVA followed by Dunnett's Multiple Comparison test was used to determine statistically significant differences between the tumor volumes of the vehicle control group and the tumor volumes of the group treated with different dosing regimens of **53**, **54** and imatinib.

Measurement of phosphorylation of eIF4E at Ser209 in tumor samples: After the final dose on day 14, tumors were excised at indicated time point and flash frozen in liquid nitrogen. The samples were homogenized in surefire lysis buffer (Perkin Elmer) supplemented with protease and phosphatase inhibitor using MS-100 Micro Smash (Tomy, Tokyo) with 1.4 mM ceramic beads for 30 seconds at 4500 rpm. The homogenate were centrifuged at 16,100 *X g* for 10mins at 4°. The protein concentration was determined using A280 measurement on the NanoDrop® 1000 spectrophotometer. The homogenates were diluted to 0.5 mg/mL with surefire lysis buffer and 4 µL was transferred to a 384-well OptiPlate™ (Perkin Elmer, Waltham, MA). To each well, 5 µL of the acceptor mix was added and incubated at room temperature for 2 h. 2 µL of donor mix was added in subdued light and the sealed plate was agitated at room

temperature for 2 h. Emission was measured using the EnVision® plate reader (Perkin Elmer, Waltham, MA). Percentage inhibition of the eIF4E phosphorylated at Ser209 is calculated based on the alphascreen signal at each time point as compared to the control at 0 h. Inhibition constants (IC_{50}) were determined by plotting the eIF4E phospho-Ser209 percentage inhibition versus log compound concentration and fitting with a non-linear regression algorhithm using GraphPad Prism (GraphPad Software Inc.).

Supporting information:

Kinase profiling data of compounds **2**, **27**, **53** and **54,** pharmacokinetic parameters of **53** and **54** in CD-1 mice and mice xenograft model, tabulated results of *in vivo* efficacy study and body weight monitoring of mice administered with **53** and **54** for 14 days QD, ^{1}H NMR spectra all final compounds, ^{13}C NMR spectra of all final compounds except **26**, **48** and **51**. This material is available free of charge *via* www.pubs.acs.org.

Author Information:

Corresponding author:

*Phone: +65-64070726; E-mail: jcherian@etc.a-star.edu.sg.

Present address:

[§]ACRA, 10 Anson Road, International Plaza #05-01/15, Singapore 079903.

[‡]GVK Biosciences Private Limited, Plot No. 28 A, IDA, Nacharam, Hyderabad, 500076, India.

[¶] IPI (Reg.No. 201108236K), 61 Biopolis Drive, #01-02, Proteos, Singapore 138673

Author Contributions

The manuscript was written through contributions of all authors. All authors have given approval to the final version of the manuscript.

Acknowledgments:

This work was financially supported by Biomedical Sciences Institutes (BMSI) and Joint Council Office (JCO Project 11 03 FG 07 05), Agency for Science, Technology and Research (A*STAR), Singapore, which is gratefully acknowledged. Both S.T.O. and S.L. are supported by the Clinician Scientist Award by the National Medical Research Council, Ministry of Health, Singapore.

We thank Mr. Laxminarayana Keetha, Mr. Seenivasa Reddy Anugu and their teams at GVK Biosciences for analog synthesis.

Abbreviations used:

BC, Blast crisis; LSC, leukemic stem cell; CML, chronic myeloid leukemia; MNK, mitogen activated protein kinase interacting kinase; eIF4E, eukaryotic translation Initiation factor 4E; CYP, cytochrome P450; MsCl, methane sulfonyl chloride.

References:

1. Waskiewicz, A. J.; Flynn, A.; Proud, C. G.; Cooper, J. A. Mitogen-activated protein kinases activate the serine/threonine kinases Mnk1 and Mnk2. *EMBO J.* **1997**, *16*, 1909-1920.

2. Scheper, G. C.; Morrice, N. A.; Kleijn, M.; Proud, C. G. The mitogen-activated protein kinase signal-integrating kinase Mnk2 is a eukaryotic initiation factor 4E kinase with high levels of basal activity in mammalian cells. *Mol. Cell. Biol.* **2001**, *21*, 743-754.

3. Ramalingam, S.; Gediya, L.; Kwegyir-Afful, A. K.; Ramamurthy, V. P.; Purushottamachar, P.; Mbatia, H.; Njar, V. C. First MNKs degrading agents block

phosphorylation of eIF4E, induce apoptosis, inhibit cell growth, migration and invasion in triple negative and Her2-overexpressing breast cancer cell lines. *Oncotarget* **2014**, *5*, 530-543.

4. Furic, L.; Rong, L.; Larsson, O.; Koumakpayi, I. H.; Yoshida, K.; Brueschke, A.; Petroulakis, E.; Robichaud, N.; Pollak, M.; Gaboury, L. A.; Pandolfi, P. P.; Saad, F.; Sonenberg, N. eIF4E phosphorylation promotes tumorigenesis and is associated with prostate cancer progression. *Proc. Natl. Acad. Sci. U. S. A.* **2010**, *107*, 14134-14139.

5. Zheng, J.; Li, J.; Xu, L.; Xie, G.; Wen, Q.; Luo, J.; Li, D.; Huang, D.; Fan, S. Phosphorylated Mnk1 and eIF4E are associated with lymph node metastasis and poor prognosis of nasopharyngeal carcinoma. *PLOS ONE* **2014**, *9*, e89220.

6. Lim, S.; Saw, T. Y.; Zhang, M.; Janes, M. R.; Nacro, K.; Hill, J.; Lim, A. Q.; Chang, C. T.; Fruman, D. A.; Rizzieri, D. A.; Tan, S. Y.; Fan, H.; Chuah, C. T. H.; Ong, S. T. Targeting of the MNK–eIF4E axis in blast crisis chronic myeloid leukemia inhibits leukemia stem cell function. *Proc. Natl. Acad. Sci. U. S. A.* **2013**, *110*, E2298-2307.

7. Wendel, H. G.; Silva, R. L.; Malina, A.; Mills, J. R.; Zhu, H.; Ueda, T.; Watanabe-Fukunaga, R.; Fukunaga, R.; Teruya-Feldstein, J.; Pelletier, J.; Lowe, S. W. Dissecting eIF4E action in tumorigenesis. *Genes Dev.* **2007**, *21*, 3232-3237.

8. Ueda, T.; Sasaki, M.; Elia, A. J.; Chio, II; Hamada, K.; Fukunaga, R.; Mak, T. W. Combined deficiency for MAP kinase-interacting kinase 1 and 2 (Mnk1 and Mnk2) delays tumor development. *Proc. Natl. Acad. Sci. U. S. A.* **2010**, *107*, 13984-13990.

9. Teo, T.; Lam, F.; Yu, M.; Yang, Y.; Basnet, S. K.; Albrecht, H.; Sykes, M. J.; Wang, S. Pharmacologic inhibition of MNKs in acute myeloid leukemia. *Mol. Pharmacol.* **2015**, *88*, 380-389.

10. Zhang, B.; Li, M.; McDonald, T.; Holyoake, T. L.; Moon, R. T.; Campana, D.; Shultz, L.; Bhatia, R. Microenvironmental protection of CML stem and progenitor cells from tyrosine kinase inhibitors through N-cadherin and Wnt-beta-catenin signaling. *Blood* **2013**, *121*, 1824-38.

11. Bhatia, R.; Holtz, M.; Niu, N.; Gray, R.; Snyder, D. S.; Sawyers, C. L.; Arber, D. A.; Slovak, M. L.; Forman, S. J. Persistence of malignant hematopoietic progenitors in chronic myelogenous leukemia patients in complete cytogenetic remission following imatinib mesylate treatment. *Blood* **2003**, *101*, 4701-4707.

12. Chu, S.; McDonald, T.; Lin, A.; Chakraborty, S.; Huang, Q.; Snyder, D. S.; Bhatia, R. Persistence of leukemia stem cells in chronic myelogenous leukemia patients in prolonged remission with imatinib treatment. *Blood* **2011**, *118*, 5565-5572.

13. Holtz, M. S.; Bhatia, R. Effect of imatinib mesylate on chronic myelogenous leukemia hematopoietic progenitor cells. *Leuk. Lymphoma* **2004**, *45*, 237-245.

14. Jamieson, C. H.; Ailles, L. E.; Dylla, S. J.; Muijtjens, M.; Jones, C.; Zehnder, J. L.; Gotlib, J.; Li, K.; Manz, M. G.; Keating, A.; Sawyers, C. L.; Weissman, I. L. Granulocyte-macrophage progenitors as candidate leukemic stem cells in blast-crisis CML. *N. Engl. J. Med.* **2004**, *351*, 657-667.

15. Druker, B. J.; Guilhot, F.; O'Brien, S. G.; Gathmann, I.; Kantarjian, H.; Gattermann, N.; Deininger, M. W.; Silver, R. T.; Goldman, J. M.; Stone, R. M.; Cervantes, F.; Hochhaus, A.;

Powell, B. L.; Gabrilove, J. L.; Rousselot, R.; Reiffers, J.; Cornelissen, J. J.; Hughes, T.; Agis, H.; Fischer, T.; Verhoef, G.; Shepherd, J.; Saglio, G.; Gratwohl, A.; Nielsen, J. L.; Radich, J. P.; SimonssonB.; Taylor, K.; Baccarani, M.; So, C.; Letvak, L.; A. Larson, R. A. Five year follow up of patients receiving imatinib for chronic myeloid leukemia. *N. Engl. J. Med.* **2006**, *355*, 2408-2417.

16. Shah, N. P.; Tran, C.; Lee, F. Y.; Chen, P.; Norris, D.; Sawyers, C. L. Overriding imatinib resistance with a novel ABL kinase inhibitor. *Science* **2004**, *305*, 399-401.

17. Weisberg, E.; Manley, P. W.; Breitenstein, W.; Brüggen, J.; Cowan-Jacob, S.W.; Ray, A.; Huntly, B.; Fabbro, D.; Fendrich, G.; Hall-Meyers, E.; Kung, A. L.; Mestan, J.; Daley G. Q.; Callahan, L.; Catley, L.; Cavazza, C.; Mohammed, A.; Neuberg, D.; Wright, R. D.; Gilliland, D. J.; Griffin, J. D. Characterization of AMN107, a selective inhibitor of wild type and mutant Bcr-Abl. *Cancer Cell* **2005**, *7*, 129-141.

18. Quintás-Cardama, A.; Vaddi, K.; Liu, P.; Manshouri, T.; Li, J.; Scherle, P. A.; Caulder, E.; Wen, X.; Li, Y.; Waeltz, P.; Rupar, M.; Burn, T.; Lo, Y.; Kelley, J.; Covington, M.; Shepard, S.; Rodgers, J. D.; Haley, P.; Kantarjian, H.; Fridman J. S.; Verstovsek, S. Preclinical characterization of the selective JAK1/2 inhibitor INCB018424: therapeutic implications for the treatment of myeloproliferative neoplasms *Blood* **2010**, *115,*3109-3117.

19. Gallipoli, P.; Cook, A.; Rhodes, S.; Hopcroft, L.; Wheadon, H.; Whetton, A. D.; Jorgensen, H. G.; Bhatia, R.; Holyoake, T. L. JAK2/STAT5 inhibition by nilotinib with ruxolitinib contributes to the elimination of CML CD34+ cells in vitro and in vivo. *Blood* **2014**, *124*, 1492-1501.

20. Bain, J.; Plater, L.; Elliott, M.; Shpiro, N.; Hastie, C. J.; McLauchlan, H.; Klevernic, I.; Arthur, J. S.; Alessi, D. R.; Cohen, P. The selectivity of protein kinase inhibitors: a further update. *Biochem. J.* **2007**, *408*, 297-315.

21. Karaman, M. W.; Herrgard, S.; Treiber, D. K.; Gallant, P.; Atteridge, C. E.; Campbell, B. T.; Chan, K. W.; Ciceri, P.; Davis, M. I.; Edeen, P. T.; Faraoni, R.; Floyd, M.; Hunt, J. P.; Lockhart, D. J.; Milanov, Z. V.; Morrison, M. J.; Pallares, G.; Patel, H. K.; Pritchard, S.; Wodicka, L. M.; Zarrinkar, P. P. A quantitative analysis of kinase inhibitor selectivity. *Nat. Biotechnol.* **2008**, *26*, 127-132.

22. Konicek, B. W.; Stephens, J. R.; McNulty, A. M.; Robichaud, N.; Peery, R. B.; Dumstorf, C. A.; Dowless, M. S.; Iversen, P. W.; Parsons, S.; Ellis, K. E.; McCann, D. J.; Pelletier, J.; Furic, L.; Yingling, J. M.; Stancato, L. F.; Sonenberg, N.; Graff, J. R. Therapeutic inhibition of MAP kinase interacting kinase blocks eukaryotic initiation factor 4E phosphorylation and suppresses outgrowth of experimental lung metastases. *Cancer Res.* **2011**, *71*, 1849-1857.

23. Diab, S.; Teo, T.; Kumarasiri, M.; Li, P.; Yu, M.; Lam, F.; Basnet, S. K. C.; Sykes, M. J.; Albrecht, H.; Milne, R.; Wang, S. Discovery of 5-(2-(phenylamino)pyrimidin-4-yl)thiazol-2(3H)-one derivatives as potent Mnk2 inhibitors: synthesis, SAR analysis and biological evaluation. *ChemMedChem* **2014**, *9*, 962–972.

24. Teo, T.; Yu, M.; Yang, Y.; Gillam, T.; Lam, F.; Sykes, M. J.; Wang, S. Pharmacologic co-inhibition of Mnks and mTORC1 synergistically suppresses proliferation and perturbs cell cycle progression in blast crisis-chronic myeloid leukemia cells. *Cancer Lett.* **2015**, *357*, 612–623.

25. Shieh, W. C.; J. M., Sclafani, J. A.; Xue, S.; Girgis, M.; Vivelo, J.; Radetich, B.; Prasad, K. Syntheses of a triad of Flt3 kinase inhibitors: from bench to pilot plant. *Org. Process Res. Dev.* **2008**, *12*, 1146-1155.

26. Shen, W.; Tremblay, M. S.; Deshmukh, V. A.; Wang, W.; Filippi, C. M.; Harb, G.; Zhang, Y. Q.; Kamireddy, A.; Baaten, J. E.; Jin, Q.; Wu, T.; Swoboda, J. G.; Cho, C. Y.; Li, J.; Laffitte, B. A.; McNamara, P.; Glynne, R.; Wu, X.; Herman, A. E.; Schultz, P. G. Small-molecule inducer of beta cell proliferation identified by high-throughput screening. *J. Am. Chem. Soc.* **2013**, *135*, 1669-1672.

27. Kato, D.; Mitsuda, S.; Ohta, H. Microbial deracemization of r-substituted carboxylic acids: substrate specificity and mechanistic investigation. *J. Org. Chem.* **2003**, *68*, 7234-7242.

28. Cherian, J.; Duraiswamy, A. J.; Nacro, K. Compounds including map kinase interacting kinases 1 and 2 (MNK1 and MNK2) modulators and ABL and ABL (T315I) inhibitors, and uses thereof. WO2014088519, June 12, 2014.

29. Lim, S.; Cherian, J.; Nacro, K.; Chew, Y. S.; Choong, M. L.; Li, L. D.; Guo, S.; Ho, M.; Joy, J.; Kwek, P.; Lee, M. A.; Liu, B.; Manoharan, V.; Ong, E.; Pendharkar, V.; Poh, Z. Y.; Poulsen, A.; Sangthongpitag, K.; Srinivararaghavan, K.; Tan, S. P.; Yang, H. Y.; Keller, T. H.; Chuah, C.; Ong, S. T.; Hill, J.; Matter, A. Dual specific inhibitors of the BCR-ABL and MNK kinases as potential therapeutics for blast crisis chronic myeloid leukemia. *Blood*, **2013**, *122* (21), 2702-2702.

30. Jauch, R.; Jakel, S.; Netter, C.; Schreiter, K.; Aicher, B.; Jackle, H.; Wahl, M. C. Crystal structures of the Mnk2 kinase domain reveal an inhibitory conformation and a zinc binding site. *Structure* **2005**, *13*, 1559-1568.

31. Zhou, T.; Commodore, L.; Huang, W. S.; Wang, Y.; Thomas, M.; Keats, J.; Xu, Q.; Rivera, V. M.; Shakespeare, W. C.; Clackson, T.; Dalgarno, D. C.; Zhu, X. Structural mechanism of the Pan-BCR-ABL inhibitor ponatinib (AP24534): lessons for overcoming kinase inhibitor resistance. *Chem. Biol. Drug Des.* **2011**, *77*, 1-11.

32. Kaminski, G. A.; Friesner, R. A.; Tirado-Rives, J.; Jorgensen, W. L. Evaluation and reparametrization of the OPLS-AA force field for proteins via comparison with accurate quantum chemical calculations on peptides. *J. Phys. Chem. B*, **2001**, *105* (28), 6474–6487.

33. Hasel, W., Hendrickson, T. F., Still, W. C. A rapid approximation to the solvent accessible surface areas of atoms. *Tetrahedron Comput. Methodol.* **1988**, *1*, 103-116.

34. Polak, E., Ribiere, G. Note sur la convergence de méthodes de directions conjuguées. Revenue francaise informat. *Recherche opérationelle, Série Rouge*, **1969**, *16*, 35-43.

35. Duraiswamy, A. J.; Lee, M. A.; Madan, B.; Ang, S. H.; Tan, E. S. T.; Cheong, W. W. V.; Ke, Z.; Pendharkar, V.; Ding, L. J.; Chew, Y. S.; Manoharan, V.; Sangthongpitag, K.; Alam, J.; Poulsen, A.; Ho, S. Y.; Virshup, D. M.; Keller, T. H. Discovery and optimization of a porcupine inhibitor. *J. Med. Chem.* **2015**, *58*, 5889−5899.

Graphical Abstract:

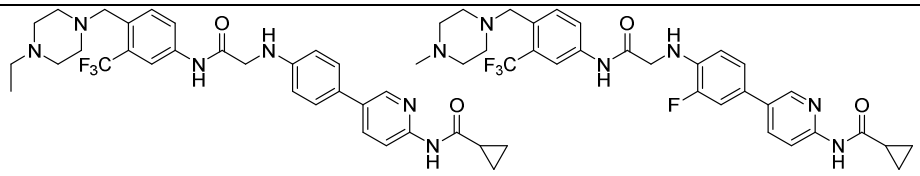

MNK1 & 2 IC_{50} (μM)	2.52 & 0.016	0.2 & 0.01
ABL1 & ABL^{T315I} IC_{50} (μM)	0.089 & 0.05	0.01 & 0.02